Chapter 4
Dielectric Properties

4.1. Introduction

A ceramic capacitor having a high capacitance is desired to have small dependences of electrostatic capacitance on the temperature and voltage for making a designation of an electric power circuit easier and a stabilization of a circuit characteristic better. Such a high capacitance material is found in a perovskite ceramic greatly used in a ceramic dielectric layer of a capacitor. For this application, a small dielectric constant dependent on the temperature and electric field field strength is desired. In order to attain a high capacitance, however, a sharp peak of dielectric constant accompanying a phase transition of perovskite ceramic is generally utilized. Because of a required higher capacitance, there will be disadvantageous that the dependence of dielectric constant on the temperature and electric field strength may be higher as dielectric constant reaches to be higher. For the purpose of obviating this problem, intensive investigations have been made for improving the temperature dependence of the dielectric constant while only a few studies have been made for improving the electric field strength dependence of the dielectric constant. Futhermore, in this experiment not only is the dependence of dielectric constant on temperature investigated but a utilization near room temperature is also experimented.

To lower the dependence of the dielectric constant on temperature is to employ relaxor materials technologically important subset of the perovskite family of ferroelectrics due to a diffuse phase transition. In a relaxor, domain wall motion and phase wall motion make a meaningful contribution to a high dielectric constant. The mechanisms (7) supporting the relaxation of dielectric polarization are

1. motion of the domain wall, the domain wall is the wall dividing a region of a crystal where all dipole or antipoles sets have the same direction. The dipoles or antidipoles(oppositely oriented polars) can exist in either 180° or 90° walls. The domain walls are an important source of dielectric loss for temperature below T_c , under applied electric field. It can be said that domain wall motion causes dissipating energy.

2. polarization-depolarization relaxation of the polar region by thermal fluctuation in an average nonpolar region;

3. motion of the boundaries of the polar regions and the boundaries of nonpolar regions under the influence of electric field.

The dielectric constant or relative permittivity (K'), dissipation factor or dielectric loss (tan δ) and dielectric strength usually determine the suitability and quality of an insulating material for electronic applications. The dielectric properties are dependent on temperature, frequency and field strength. Under the influence of an applied electric field, the short-range displacements of charge carriers lead to the storage of electrical energy which is proportional to the dielectric constant.

The charging current leads the applied voltage by 90° in an ideal dielectric. However, the phase angle of real materials is impeded such that the current leads the voltage by 90°-δ where δ is the retarding angle. This loss current arises from the dissipation of energy associated with rotation or oscillation of dipoles which is called loss tangent or dissipation factor

Dissipation factor represents the relative expense of energy to obtain a given amount of charge storage, generally taken as an indication of the quality of a capacitor. A high loss is undesirable in all applications. It lowers the quality factor and also generates the heat resulting the electrical

conductivity. For high K' dielectrics with no antiferroelectric phase the dissipation factor correlated drastically with the domain wall movement. This can occur from a perovskite ceramic such as $BaTiO_3$ and $PbTiO_3$.

Porosity results in internal surfaces that are an important source of loss because the surfaces of ceramics contain a high concentration of defects due to the transition from a solid crystal to a gas phase. If the surface of ceramics containing high pores is subjected to external atmosphere , moisture can take in it and result in an increase in loss, particularly if soluble ions are leached from the solid phase. Therefore, a dence pore free ceramic is desired to obtain a low loss (4).

The loss due to conductivity is increased at low frequencies but in the kilohertz region and above, it can be negligible. Because there is a shift of charge carriers, such as vacant oxygen sites as well as electrocs at the low frequencies. The loss at high frequencies can be kept down by increasing the electrode thickness. To improve this problem is to use a low resistivity metal. The element of Group IB (Ag and Au) have a valence of one among the best conductors known and the most widely used in electronics. In this work, silver is the selected electrode because of the low cost and good conductor (27).

The dielectric constant and dielectric loss of relaxor materials are strongly dependent on temperature, frequency and field strength. Use of relaxor ferroelectrics is advantageous in that a high capacitance can be obtained over a wider temperature range with small dependence of electrostatic capacitance on the temperature and frequency than those of conventional ceramic capacitors. Therefore, use of the capacitor according to relaxor behavior is advantageous. For example, a power source device for

mounting on a stationary artificial sattelite is exposed to periodically fluctuating temperature between -20 °C and 50 °C and subjected to voltage application. Use of these capacitors in filter circuit in such device is advantageous in that the power source devices gets a high stability and that the number of capacitors to be used can be decreased leading to reduction of the mounting area and reduction of the weight as well as the reduction of the cost.

The dielectric loss (ε'' or K'') generally similar temperature behavior to the dielectric constant (ε' or K') and phase transition that changes with temperature can be determined by dielectric measurements. These measurements are particularly straighforward with impedance bridges which separate the conductance and capacitance of the crystals.

Measurements are usually made as a function of temperature, frequency, dc bias or pressure. In this study the purposes of these experiments were concerned with; the change of K' and K'', as functions of temperature and frequency.

The first aim was to investigate the transition temperature of BNT and 0.90BNT-0.10PT from room temperature to 500 °C. From previous studies (11,20,36) observed from room temperarure to 500 °C, BNT was ferroelectric at room temperature (12). Above 200 °C it transformed to an antiferroelectric state in which it remained up to 320 °C (11), the Curie temperature at which a dielectric constant maximum could be observed ($K' \approx$ 2000). At this point, the broad K' was also seen. Above the Curie temperature the phase paraelectric of K' gradually fell. In this study the phase transition temperatures of both BNT and 0.90BNT-0.10PT systems doped with Ba^{2+} cation were observed. The K' and dissipation factor (K") of

these compositions doped were measured as a function of temperature. The effect of Ba on the K' and dissipation factor as well as the transition was investigated.

The second aim was to consider the effect of frequency and %Ba dopant on the K', the dissipation factor and the transition temperature .

4.2. Procedure and Apparatus

The samples were measured by vernier calipers in both diameter and thickness. Then the samples were painted with silver paste as an electrode and fired at 700 °C. The fired sample was put on the sample holder as shown in Fig.24. A diagram of the apparatus is shown in Fig.25. The capacitance and dissipation factor were collected every 5 °C with increasing temperature at 2 °C/min from room temperature to 500 °C. The measurements were made with HP 4192A LF Impedance Analyzer at different frequencies, 1,10,100 kHz and 1 MHz, respectively.

4.3. Results and Discussion

The results of K' for BNT, 5%, 10% and 15% Ba doped BNT at different sintering temperatures are shown in Fig.26-28 and Fig.32.

An increase in the amount of Ba dopant can reduce grain growth resulting in higher dielectric constant(K'), as seen in Fig.32. The effect of grain size impacts on the dielectric properties of ceramics. In finely grained $BaTiO_3$, 90° twins are absent, giving rise to internal stress and increase polarization. The degree of 90° twinning increases with grain size. These twins in corsed grained $BaTiO_3$ relieve the stress and cause a lower dielectric

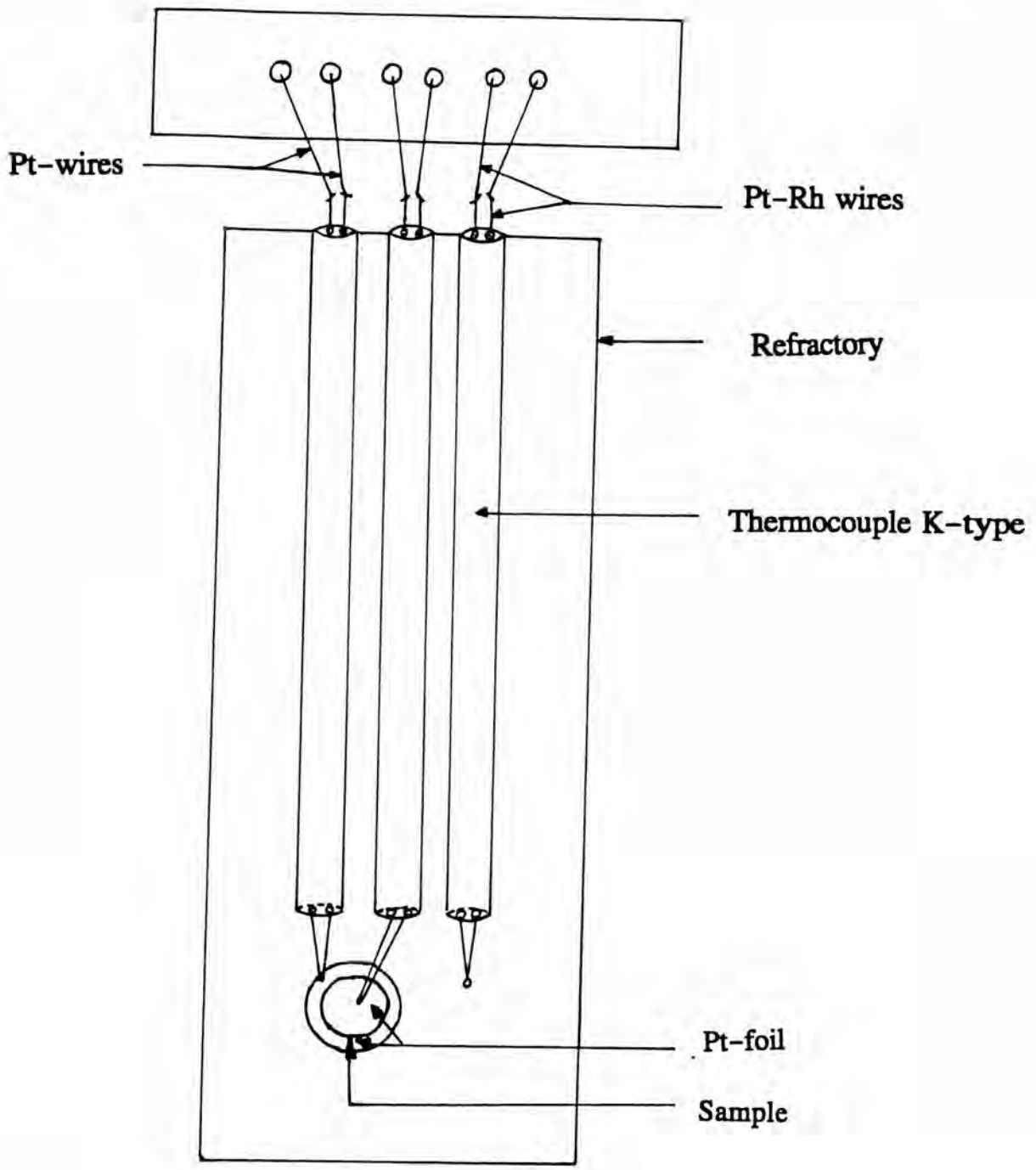

Fig.24 Sample holder for the capacitance and dissipation factor measurements

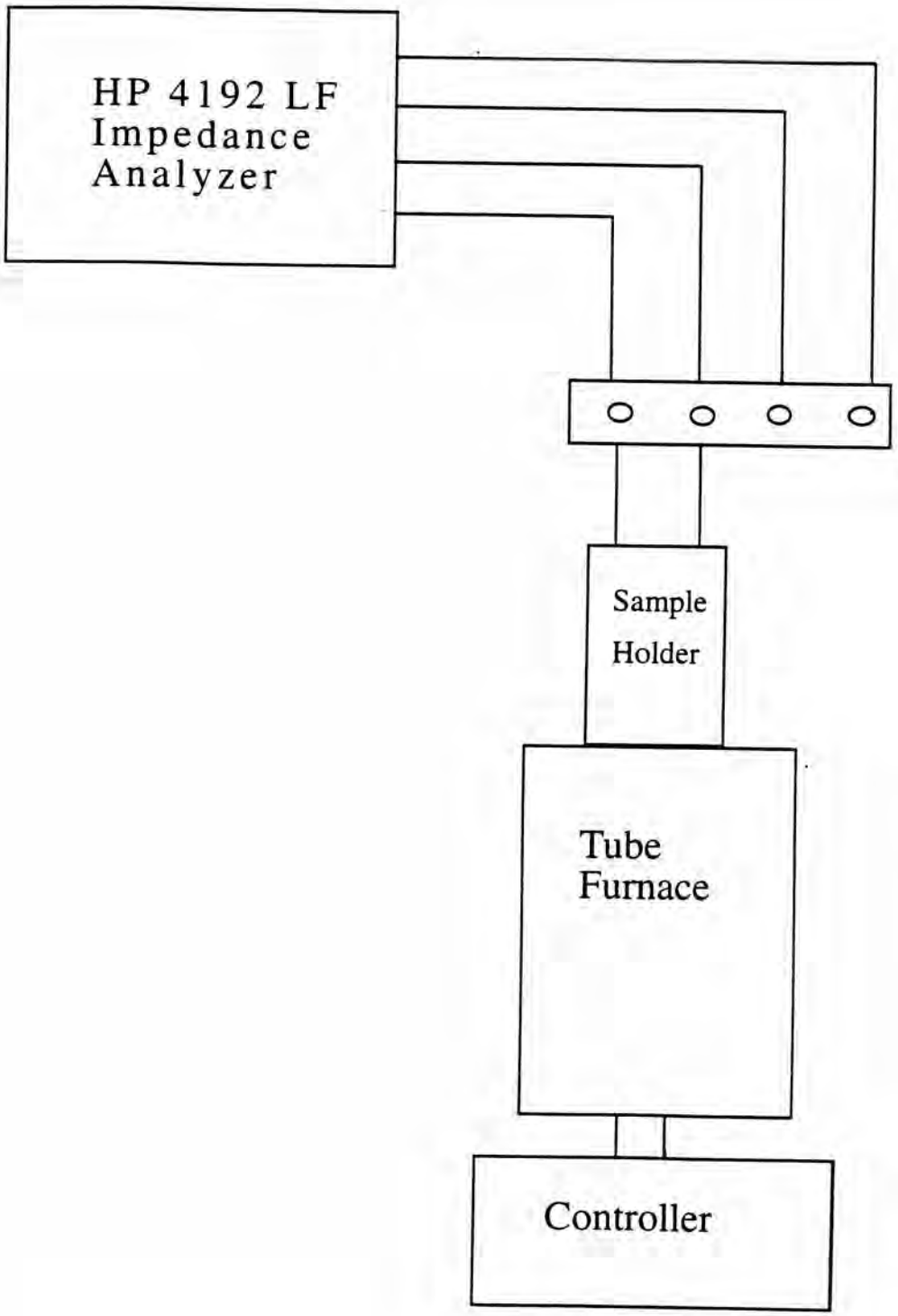

Fig.25 Diagram of apparatus used for the capacitance and dissipation factor measurements at high temperature.

constant (32). The highest K' of this material can be obtained by controlling a uniform, small grain size and highest density. That the relationship between dielectric and grain size can be seen in the results of the microstructure for Ba doped BNT are shown in Fig.11 and Fig.27. They show that the addition of Ba in BNT inhibits grain growth and small grains give a higher dielectric constant. In Fig.32 it depicts the effect of second phase at 15% Ba doped BNT that affects the K' of this composition at 1175 °C. It should be the second phases that make the K' lower. In addition, these results from dielectric data indicate a strong relaxor characteristic of Ba doped BNT because the dielectric constant at the first transition temperature shifts to higher temperature with increasing the frequency. Most of the compositions show a diffuse phase transition with a strong frequency dispersion. The first transition temperature decreases close to room temperature at 5 %Ba but with a further addition of Ba to 10% and 15% it change insignificantly. The reason is that the Curie temperature of $BaTiO_3$ (120-130 °C) (29) is lower than that of BNT (220 °C) (6) such that the first transition temperature can be shifted to lower temperature. The results collected in Table 8-9, shows a maximum K', first and second transition temperature for Ba doped BNT and Ba doped 0.90BNT-0.10PT as a function of compositions and sintering temperature. It is observed distinctly in the case of 5% Ba doped BNT compared with undoped BNT at the sintering temperature of 1175 °C. The first transition temperatures is lowered from 170 to 72 °C. With increasing %Ba to 10% and 15%, the first transition temperatures insignificantly change since an amount of Ba dopant does not impact on the transition temperature. As the Ba content increases, dielectric loss also increases depicted in Fig.34. Regarding with both dissipation factor and dielectric constant as shown in Fig.32 and Fig.34, it is found that 5% Ba doped BNT is the good condition to employ properly in very wide range of temperature, from room temperature to 400 °C, according with acceptable

dissipation factor kept below 0.05 and 10%Ba doped BNT is also a good selection in the case of higher K' than 5% Ba doped BNT.

Like Ba doped BNT at 1150 °C and 1200 °C, max K' of Ba doped BNT at 1175 °C gives higher as %Ba increases and the dielectric constant at the room temperature also increases by the factor of 2 for 5% Ba doped BNT as compared with the undoped BNT. This probably because of the high dielectric constant of Ba expected from $BaTiO_3$, and the smaller grain size. At 15% Ba doped BNT, however, max K' decreases in a few quantity relevant to the result of microstructure, as shown in Fig.11(d). Clearly, there is a second phase affecting the dielectric constant and this second phase results in an increased dielectric loss and a decreased dielectric constant. For a trend of Ba doped BNT at 1200 °C the results of max K', first transition temperature are higher and lower, respectively as %Ba increases as same as those of Ba doped BNT at 1150 °C and 1175 °C. Although, in this experiment, %Ba doped BNT is up to 15%, it is still have relaxor behavior, a diffuse phase transition with a strong frequency dispersion. In disagreement with the dielectric properties of Ba doped BNT relaxor reported by Takenaka (18), the dielectric constant data showed a morphotropic phase boundary (MPB) exiting at 6-7% Ba doped BNT. That is, the first transition temperature does not appear at the Ba content more than MPB, so called, no longer relaxor behavior. The reason is that there is a difference of calcination temperature in that Takenaka (18) calcined the powder at 800 °C but in this work the calcined powder was prepared at 850 °C.

With considering the effect of the sintering temperature, the dissipation factor and the first transition temperature are nearly independence of the sintering temperature as depicted in Fig.33 and Table 8 but the dielectric constant of most compositions increases as the sintering temperature

increases, as shown in Fig.33. As the sintering temperature increases grian size increases but the max K' still increases. It may be an other effect such as density and porosity are more influenced than a smaller grain size (29) with an increase of %Ba dopant.

The results of change in dielectric constant for Ba doped 0.90 BNT-0.10 PT as a function of an amount of dopant at 100 kHz are shown in Fig.35. The max K' increases for 5% Ba doped in this system when compared with undoped materials and decreases as %Ba is further. In this system, the frequency at 1 kHz are not interesting since at 10% Ba doped 0.90BNT-0.10PT the dielectric constant decreases at 10, 100 kHz and 1 MHz but at 1 kHz conductivity gives an anomalously higher dielectric constant agreed with the results of the dissipation factor, as shown in Fig.29(b), Fig.30(c) and Fig.31(c). It can be seen that the characteristics of these results are different from those of other compositions. In addition, the dissipation factor of Ba doped 0.90BNT-0.10PT system is likely constant as functions of %Ba and sintering temperature, as depicted in Fig.37 and Fig.38. The K' at room temperature also increases by a factor of about 2 times for 5% Ba doped 0.90 BNT-0.10PT as compared with undoped materials which is a few higher than that of Ba doped BNT system since the K' at room temperature of undoped small lead content is higher than that of undoped BNT. With 10% Ba the first transition disappears and the K' lowers explained by the phase transformation and the appearance of the second phase which limits the formation of domain and causes a decrease of the dielectric constant. In relevance to the results of dielectric properties of Ba doped 0.90 BNT-0.10 PT made by Kuharuangrong (6), 5% Ba doped in this based solid solution results in the increase of dielectric constant at the maximum and also at the first transition temperature. A phase boundary or MPB of this system is in between 5-10% Ba easily observed by the disappearance of the first

transition temperature, no evidence of relaxor behavior. It implies that the structure may be ordered or lack local variations in stoichiometry resulting in large random electric field which may be at the origin of the relaxor behavior. With the addition of Ba, for example, at 1175 °C the first transition temperature of this material decreases as compared with undoped composition giving a broad phase region from ferroelectric to antiferroelectric, as collected in Table 6. The reason is that there are many types of elements exist in A-site of this perovskite solid solution. Such many types of the elements; Bi, Na and Pb make a composition and temperature more disordered or fluctuated so that the transition temperature can be broadened. In similar to the result obtained from $Pb(Mg_{1/3}Ta_{2/3})O_3$ (PMT) - $PbTiO_3$ (PT) - $BaTiO_3$ (BT) system, Kim' s work (33) the composition of 0.6PMT-0.35PT-0.05BT or 5% doped 0.60PMT-0.35PT showed a broad maxima of dielectric constant and an increase in transition temperature with increasing frequency. In addition, the max K' decreases gradually with an increase of %Ba. Like 5% Ba doped 0.90BNT-0.10PT, the dielectric constant at room temperature increases by the factor of about 2 times for 5% Ba doping in 0.60PMT-0.35PT as compared with the undoped system. Unlike the results of Ba doped 0.90BNT-0.10PT as listed Table 9, the two transition temperatures of that system decreased gradually with the addition of %Ba and grain size of Ba doped 0.60PMT-0.35PT increased with increasing in an amount of $BaTiO_3$.

Distinctly, the sample sintered at 1200 °C of 5% Ba doped 0.90BNT-0.10PT differed from the data of sintered sample at 1150 and 1175 °C as shown in Fig.36 in that the first transition temperature of the sample at 1200 °C sintering temperature is ambiguous and not clear. It may be present or not. It is hard to investigate. Its characteristics looks like 10% Ba doped

0.90BNT-0.10PT but the value of the dielectric constant at room temperature is higher.

When compared with Ba doped BNT, Ba doped 0.90BNT-0.10PT has a higher dielectric constant both at room temperature and Curie temperature , as seen in Fig.33 because there is Pb $^{2+}$ playing a role on increasing max K'. The Pb cation has a lone pair s2 ion (34) contributing to polar distortion giving a higher max K'. In addition, the second transition temperatures of Ba doped 0.90BNT-0.10PT is higher than those of Ba doped BNT because $PbTiO_3$ resulting from Pb^{2+} has a high Curie temperature (T_c = 493 ^{o}C) (1) Therefore, this system, especially with small $PbTiO_3$ content, 5% Pb is important to apply in high temperature device. In addition, the K' at room temperature of Ba doped 0.90BNT-0.10PT system is higher and the most important thing for this system is the lower first transition temperature. Such a lower first transition temperature makes an antiferroelectric phase more broadened. Moreover, the grain size of this system is larger than that of Ba doped BNT. Although, the more the grain size the more the dielectric constant. The reason should be the influence of lead content that play a role more than the influence of a smaller grain size in Ba doped BNT.

Table 6. Maximum K', the first and Curie temperature for Ba doped $Bi_{0.5}Na_{0.5}TiO_3$ as functions of frequencies and compositions at 1175 °C.

$Bi_{0.5}Na_{0.5}TiO_3$

Frequency (kHz)	Maximum K'	T_{t1} (°C)	T_{t2} (°C)
1	2540	170	350
10	2540	177	350
100	2540	188	350
1000	2540	190	350

0.95 $Bi_{0.5}Na_{0.5}TiO_3$ - 0.05 $BaTiO_3$

Frequency (kHz)	Maximum K'	T_{t1} (°C)	T_{t2} (°C)
1	3560	72	292
10	3500	75	292
100	3500	77	292
1000	3600	80	292

0.90 $Bi_{0.5}Na_{0.5}TiO_3$ - 0.10 $BaTiO_3$

Frequency (kHz)	Maximum K'	T_{t1} (°C)	T_{t2} (°C)
1	4550	72	295
10	4495	78	295
100	4495	83	295
1000	4650	-	295

0.85 $Bi_{0.5}Na_{0.5}TiO_3$ - 0.15 $BaTiO_3$

Frequency (kHz)	Maximum K'	T_{t1} (°C)	T_{t2} (°C)
1	4330	77	298
10	4300	79	298
100	4300	82	298
1000	4480	-	298

Table 7. Maximum K', the first and Curie temperature for Ba doped 0.90BNT - 0.10PT as functions of frequencies and compositions at 1175 °C.

$0.90Bi_{0.5}Na_{0.5}TiO_3$ - 0.10 $PbTiO_3$

Frequency (kHz)	Maximum K'	T_{t1} (°C)	T_{t2} (°C)
1	5880	152	316
10	5800	152	316
100	5800	153	316
1000	5800	153	316

$0.95(0.90Bi_{0.5}Na_{0.5}TiO_3$ - 0.10 $PbTiO_3)$-0.05 $BaTiO_3$

Frequency (kHz)	Maximum K'	T_{t1} (°C)	T_{t2} (°C)
1	6100	68	325
10	6050	73	325
100	6000	79	325
1000	6150	88	325

$0.90(0.90Bi_{0.5}Na_{0.5}TiO_3$ - 0.10 $PbTiO_3)$-0.10 $BaTiO_3$

Frequency (kHz)	Maximum K'	T_{t1} (°C)	T_{t2} (°C)
1	6500	-	325
10	5780	-	325
100	5600	-	325
1000	5880	-	325

0.85 $(0.90Bi_{0.5}Na_{0.5}TiO_3$ - 0.10 $PbTiO_3)$-0.15 $BaTiO_3$

Frequency (kHz)	Maximum K'	T_{t1} (°C)	T_{t2} (°C)
1	5800	-	325
10	5700	-	325
100	5700	-	325
1000	5900	-	325

Table 8. Maximum K' , the first and Curie temperature for Ba doped $Bi_{0.5}Na_{0.5}TiO_3$ as functions of compositions and sintering temperatures at 1 kHz.

1150 °C

Compositions	Maximum K'	T_{t1} (°C)	T_{t2} (°C)
BNT	-	-	-
BNT-5BaT	3560	70	290
BNT-10BaT	4250	68	295
BNT-15BaT	4480	69	288

1175 °C

Compositions	Maximum K'	T_{t1} (°C)	T_{t2} (°C)
BNT	2450	170	350
BNT-5BaT	3560	72	292
BNT-10BaT	4550	72	295
BNT-15BaT	4300	77	298

1200 °C

Compositions	Maximum K'	T_{t1} (°C)	T_{t2} (°C)
BNT	2580	192	335
BNT-5BaT	3700	125	300
BNT-10BaT	4560	72	310
BNT-15BaT	4980	80	295

Table 9. Maximum K' , the first and Curie temperature for Ba doped $0.90Bi_{0.5}Na_{0.5}TiO_3$ - 0.10 $PbTiO_3$ as functions of compositions and sintering temperatures at 100 kHz

1150 °C

Compositions	Maximum K'	T_{t1} (°C)	T_{t2} (°C)
BNT10PT	-	-	-
BNT10PT-5BaT	6050	75	316
BNT10PT-10BaT	5450	-	325
BNT10PT-15BaT	5200	-	330

1175 °C

Compositions	Maximum K'	T_{t1} (°C)	T_{t2} (°C)
BNT10PT	5880	152	316
BNT10PT-5BaT	6000	78	325
BNT10PT-10BaT	5650	-	327
BNT10PT-15BaT	5650	-	323

1200 °C

Compositions	Maximum K'	T_{t1} (°C)	T_{t2} (°C)
BNT10PT	6200	146	306
BNT10PT-5BaT	5950	-*	325
BNT10PT-10BaT	6250	-	327
BNT10PT-15BaT	5950	-	325

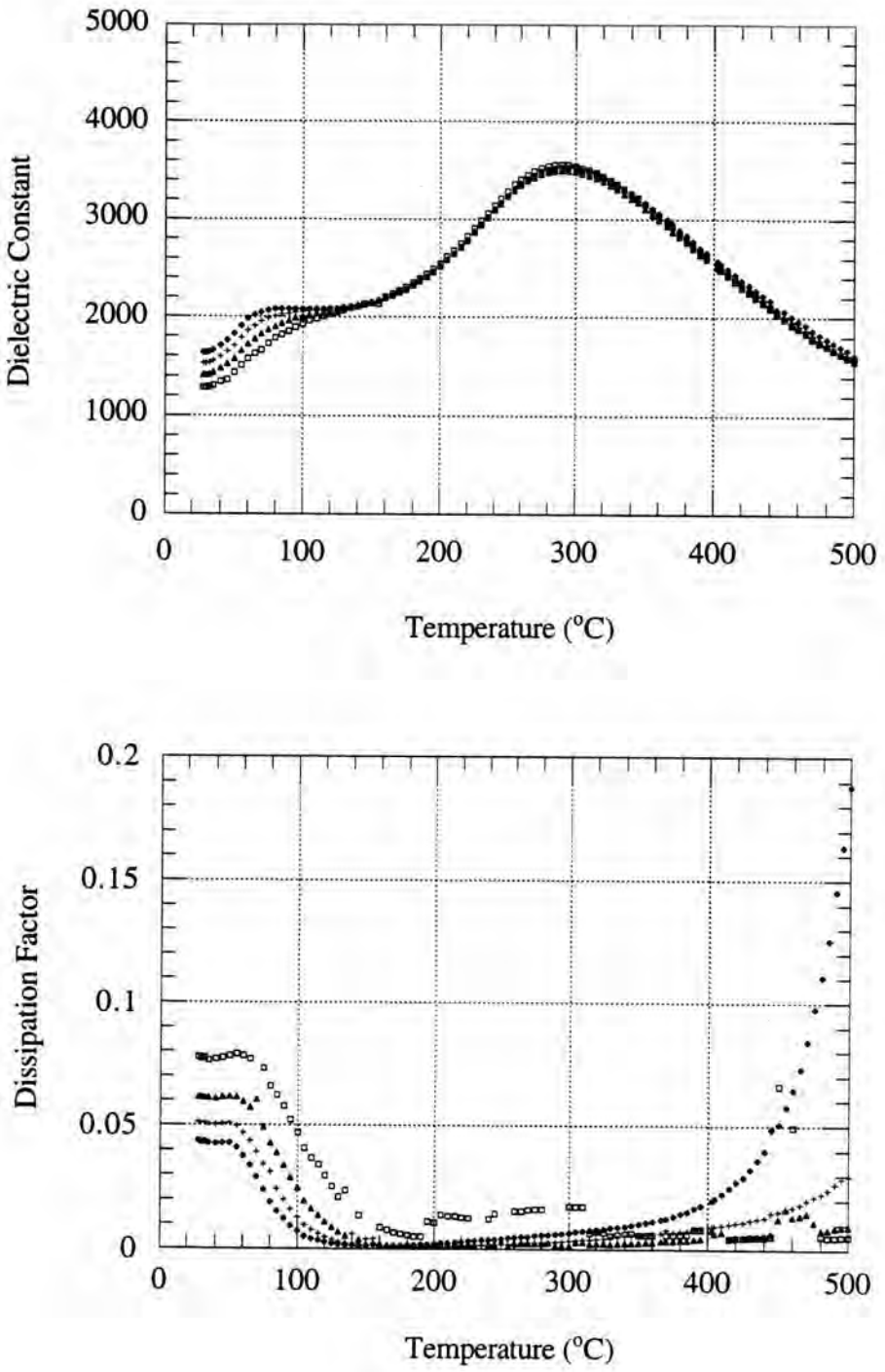

(a)

Fig.26 Change in dielectric constant and dissipation factor of (1-x)BNT-xBaT at different frequencies at 1150 °C (a) x = 0.05 (b) x = 0.10 (c) x =0.15 ♦ for 1 kHz, + for 10 kHz, ▲ for 100 kHz, □ for 1 MHz

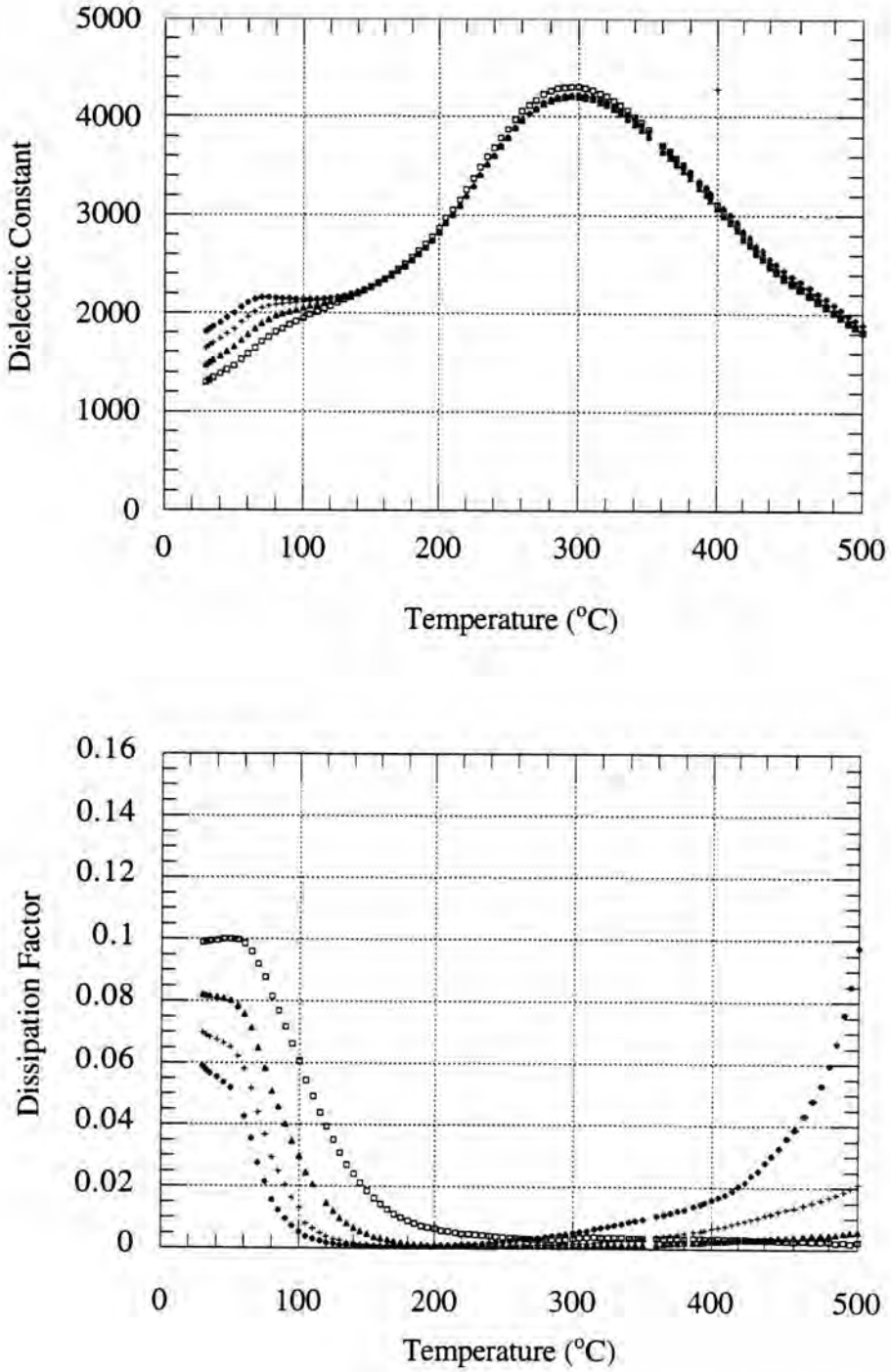

Fig.26(b) 0.90BNT-0.10BaT at 1150 °C ♦ for 1 kHz, + for 10 kHz, ▲ for 100 kHz, □ for 1 MHz

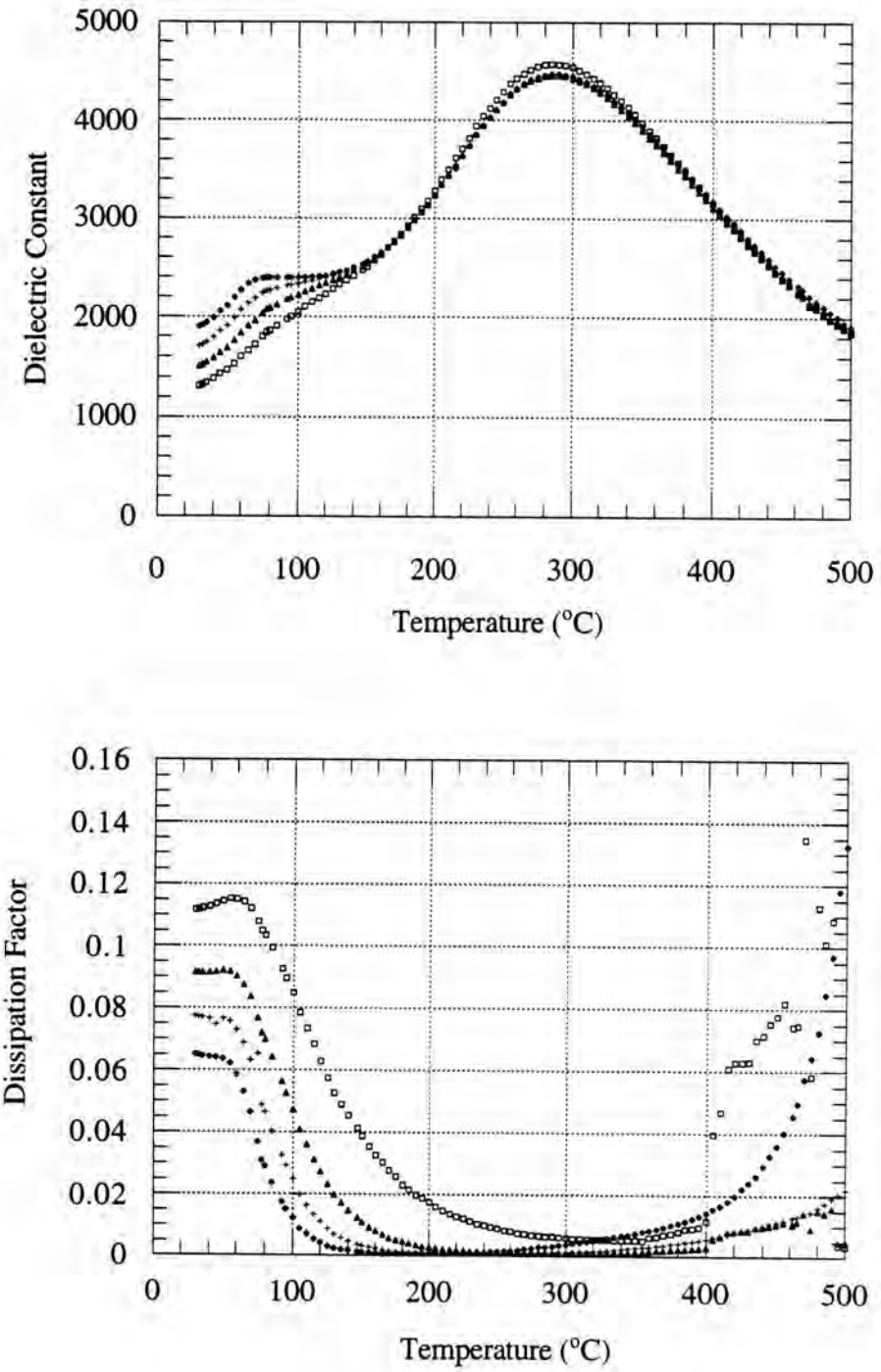

Fig.26(c) 0.85BNT-0.15BaT at 1150 °C ♦ for 1 kHz, + for 10 kHz, ▲ for 100 kHz, □ for 1 MHz

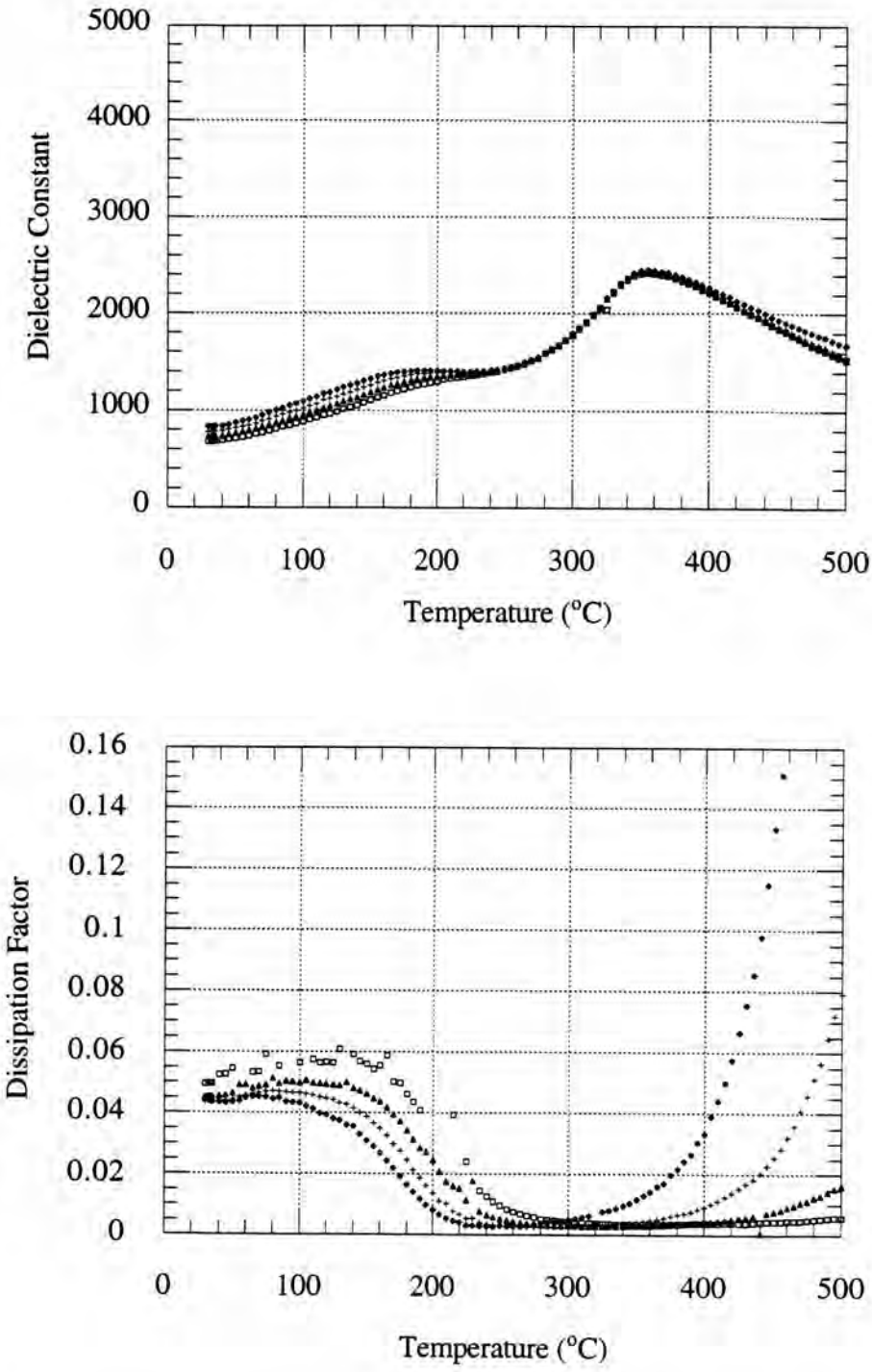

(a)

Fig.27 Change in dielectric constant and dissipation factor of (1-x)BNT-xBaT at different frequencies at 1175 °C (a) x = 0.0 (b) x = 0.05 (c) x = 0.10 (d) x = 0.15 ♦ for 1 kHz, + for 10 kHz, ▲ for 100 kHz, □ for 1 MHz

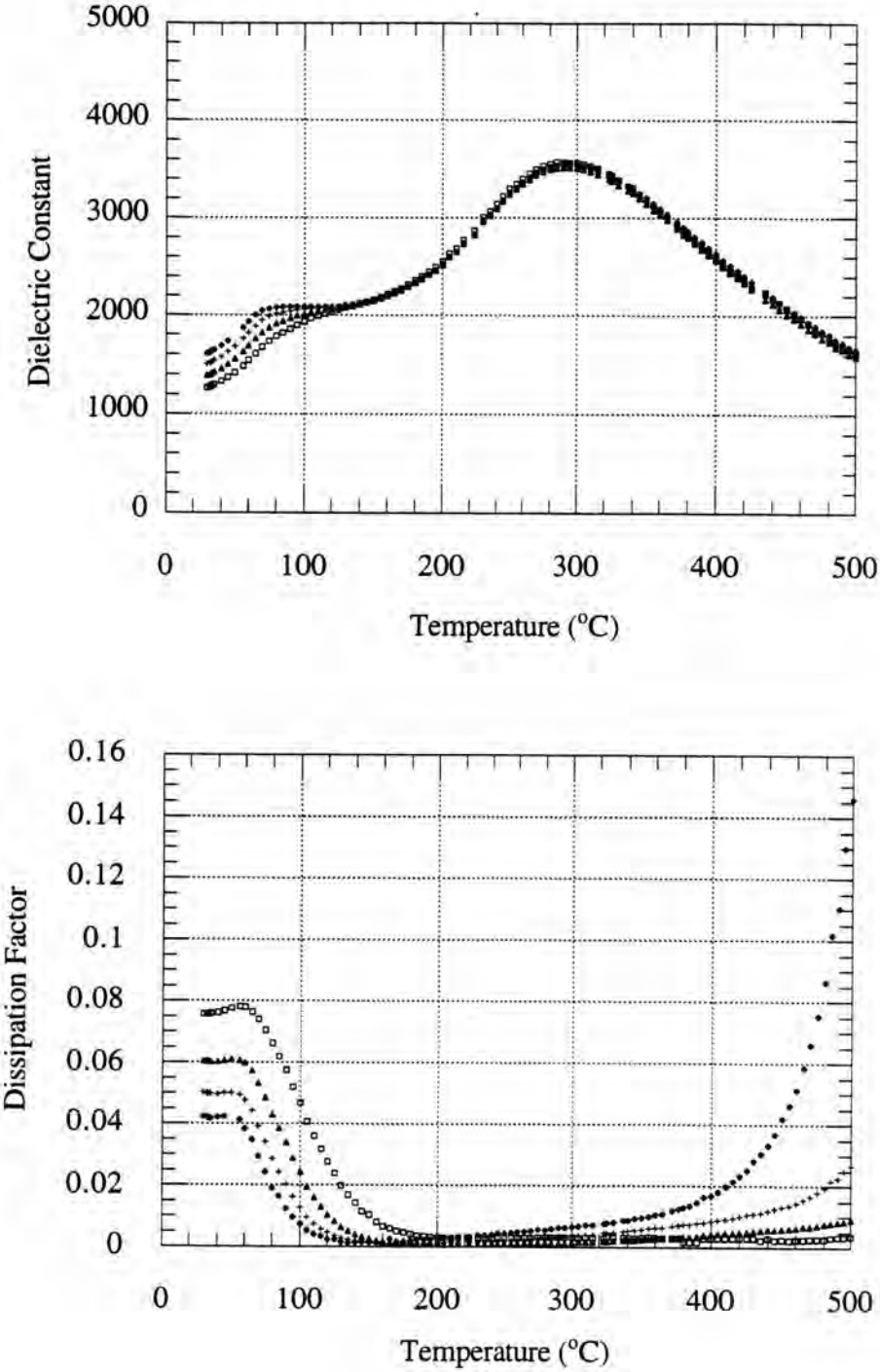

Fig.27(b) 0.95BNT-0.05BaT at 1175 °C ♦ for 1 kHz, + for 10 kHz, ▲ for 100 kHz, □ for 1 MHz

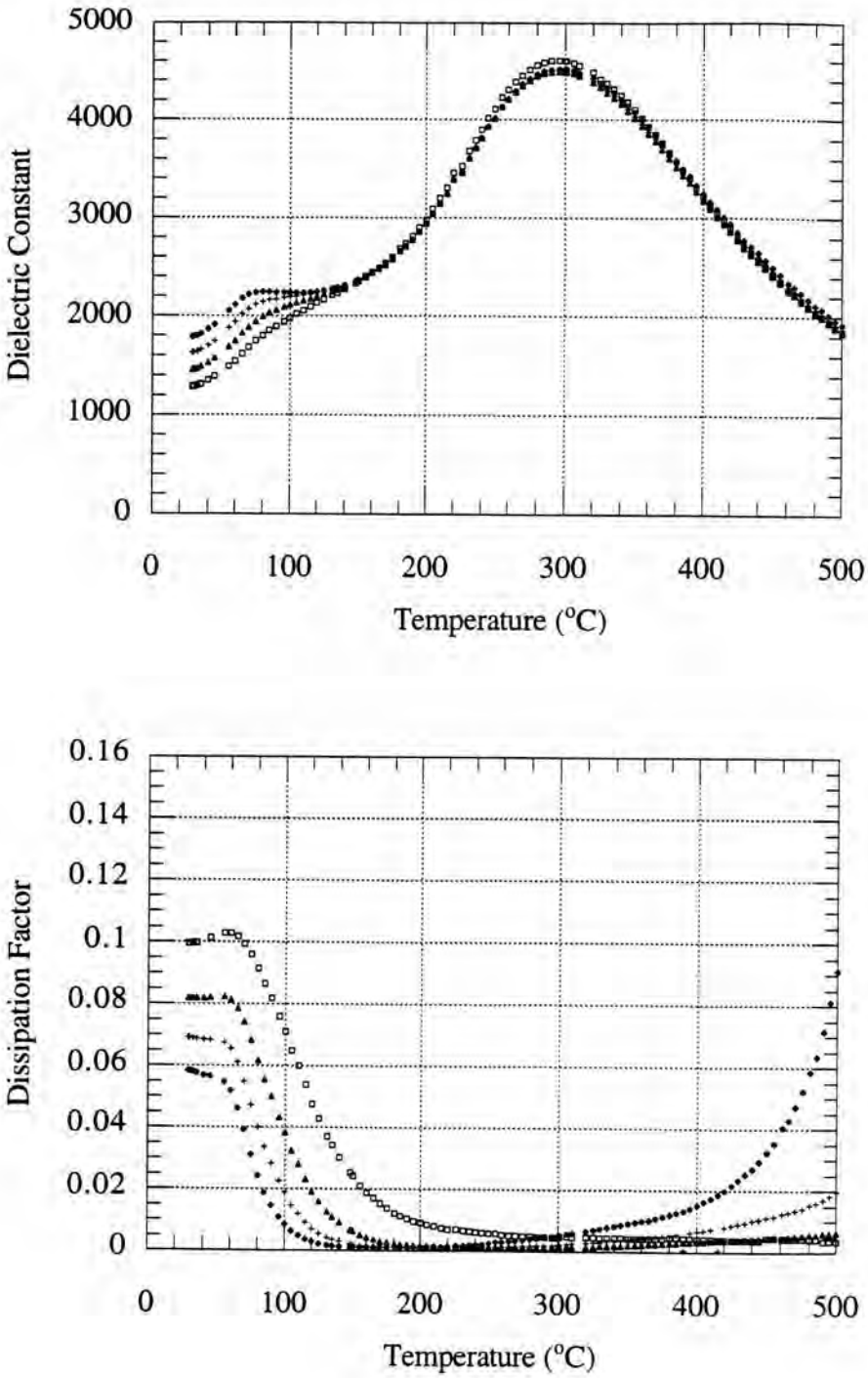

Fig.27(c) 0.90BNT-0.10BaT at 1175 °C ♦ for 1 kHz, + for 10 kHz, ▲ for 100 kHz, □ for 1 MHz

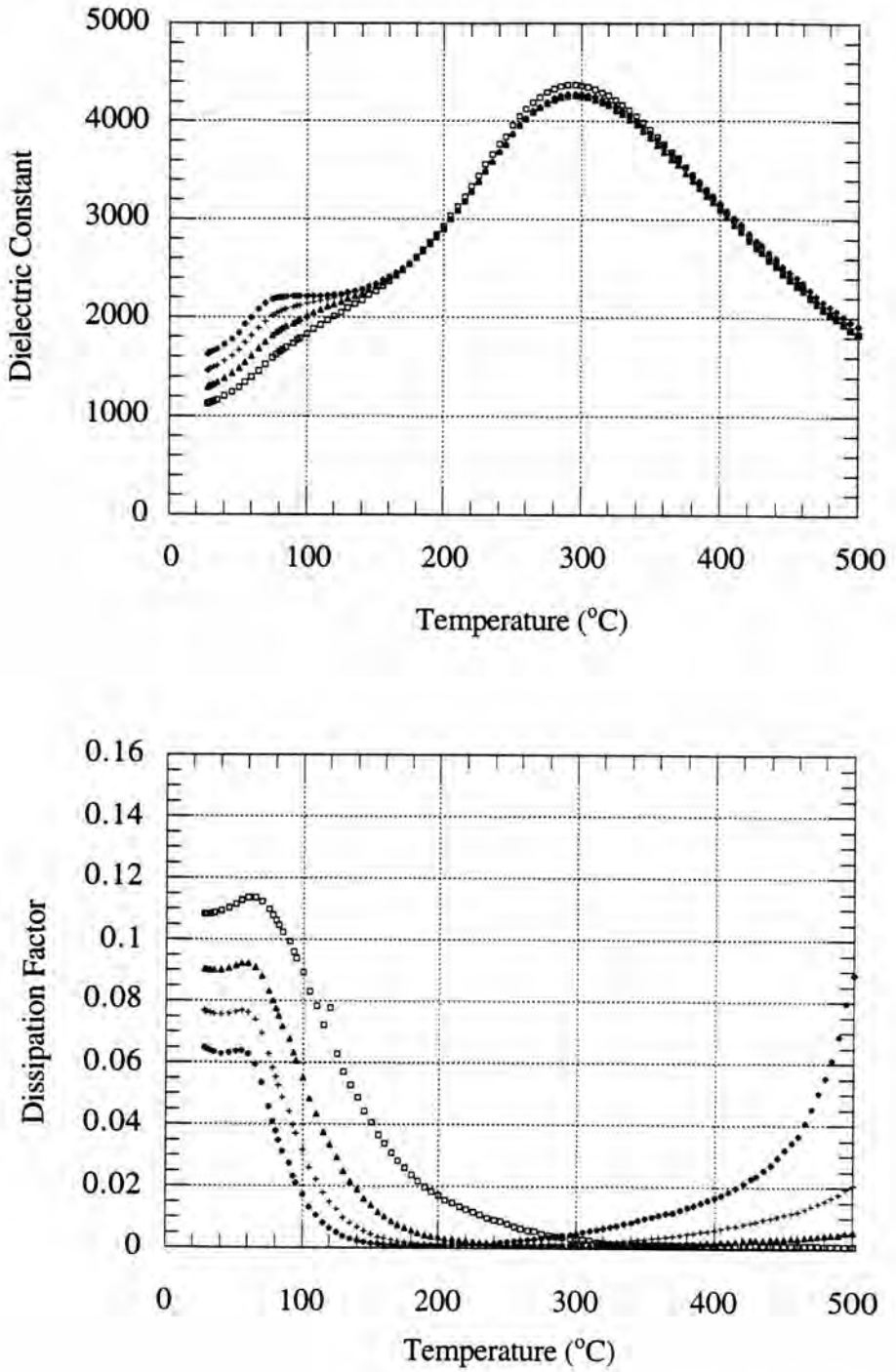

Fig.27(d) 0.85BNT-0.15BaT at 1175 °C ♦ for 1 kHz, + for 10 kHz, ▲ for 100 kHz, □ for 1 MHz

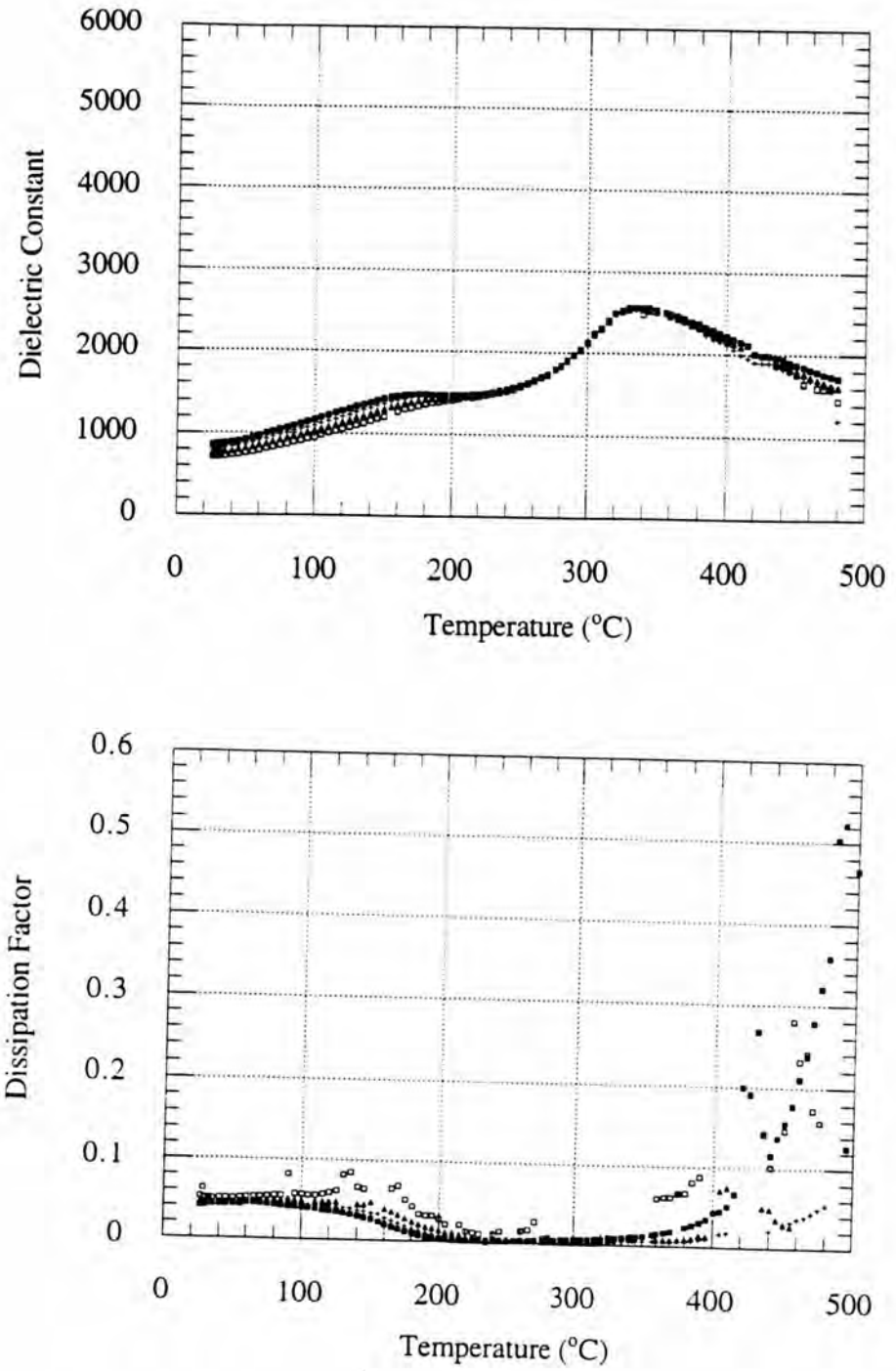

(a)

Fig.28 Change in dielectric constant and dissipation factor of (1-x)BNT-xBaT at different frequencies at 1200 °C (a) x = 0.0 (b) x = 0.05 (c) x = 0.10 (d) x = 0.15 ♦ for 1 kHz, + for 10kHz, ▲ for 100kHz, □ for 1 MHz

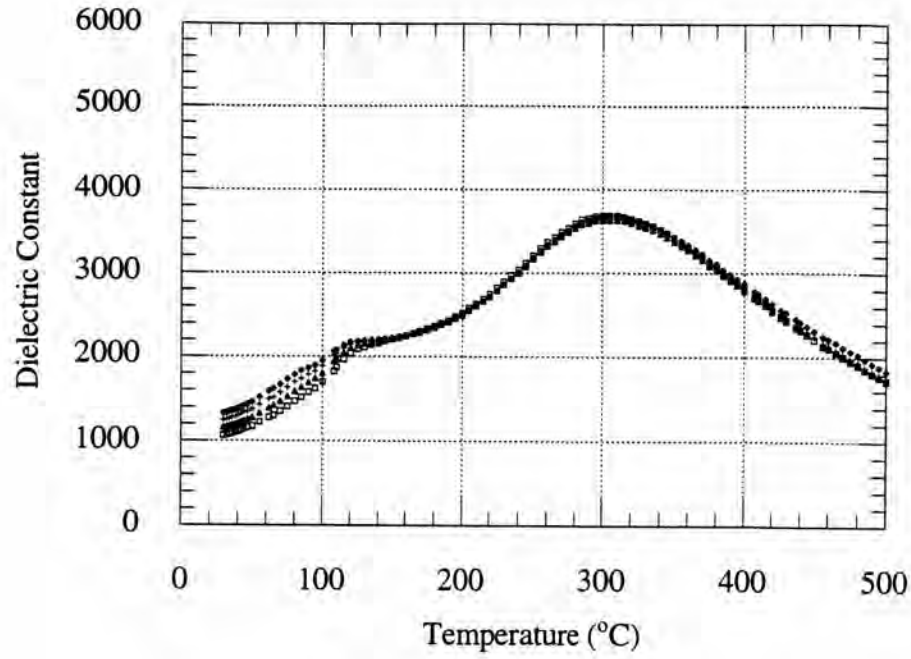

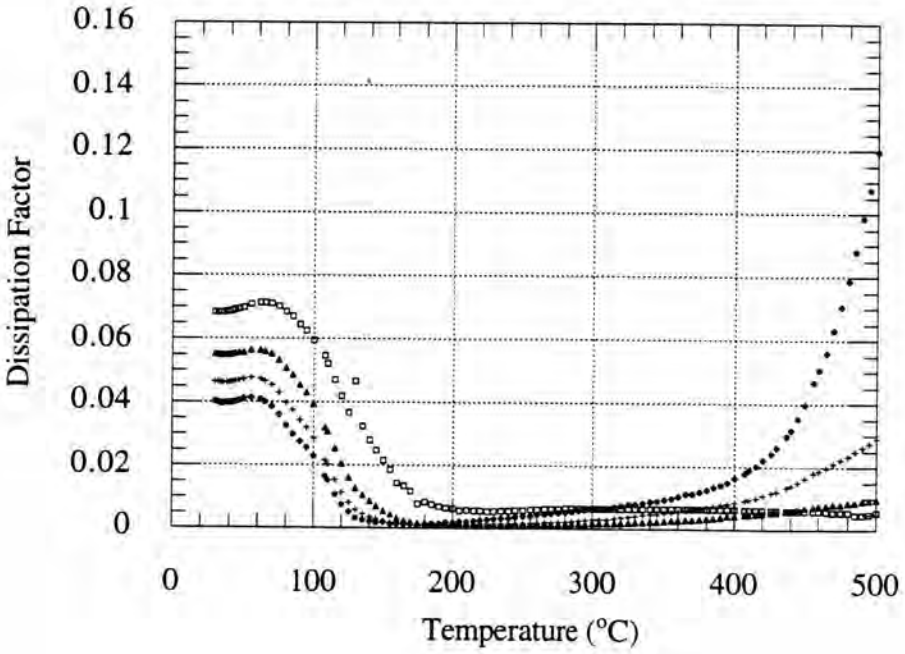

Fig.28(b) 0.95BNT-0.05BaT at 1200 °C ♦ for 1 kHz, + for 10 kHz, ▲ for 100 kHz, □ for 1 MHz

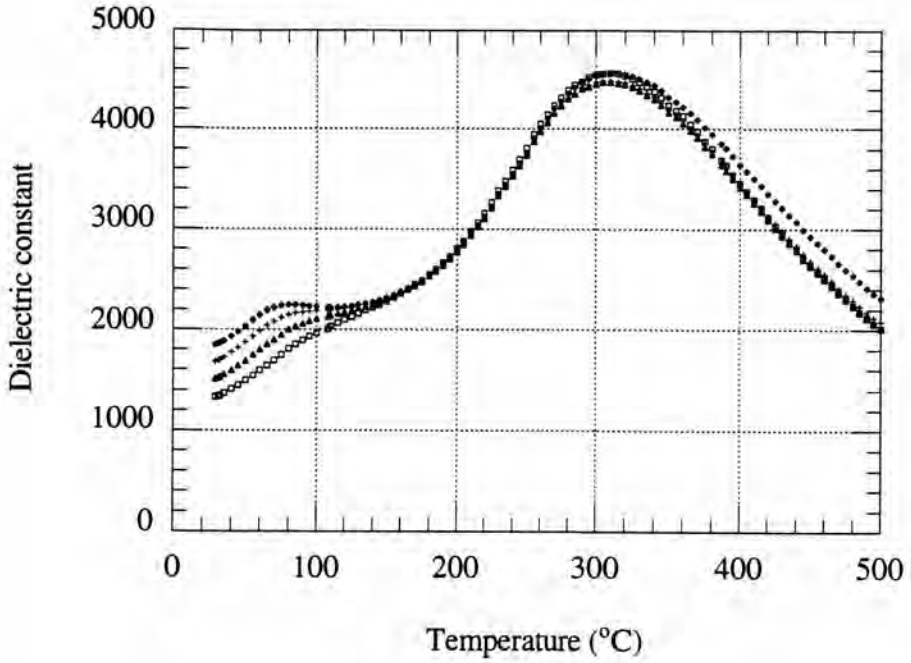

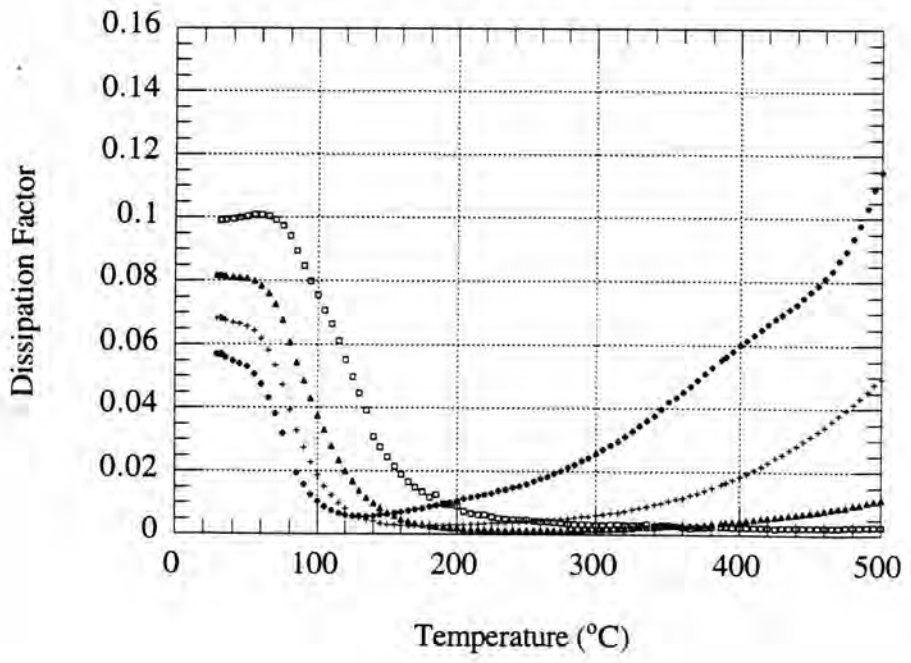

Fig.28(c) 0.90BNT-0.10BaT at 1200 °C ♦ for 1 kHz, + for 10 kHz, ▲ for 100 kHz, □ for 1 MHz

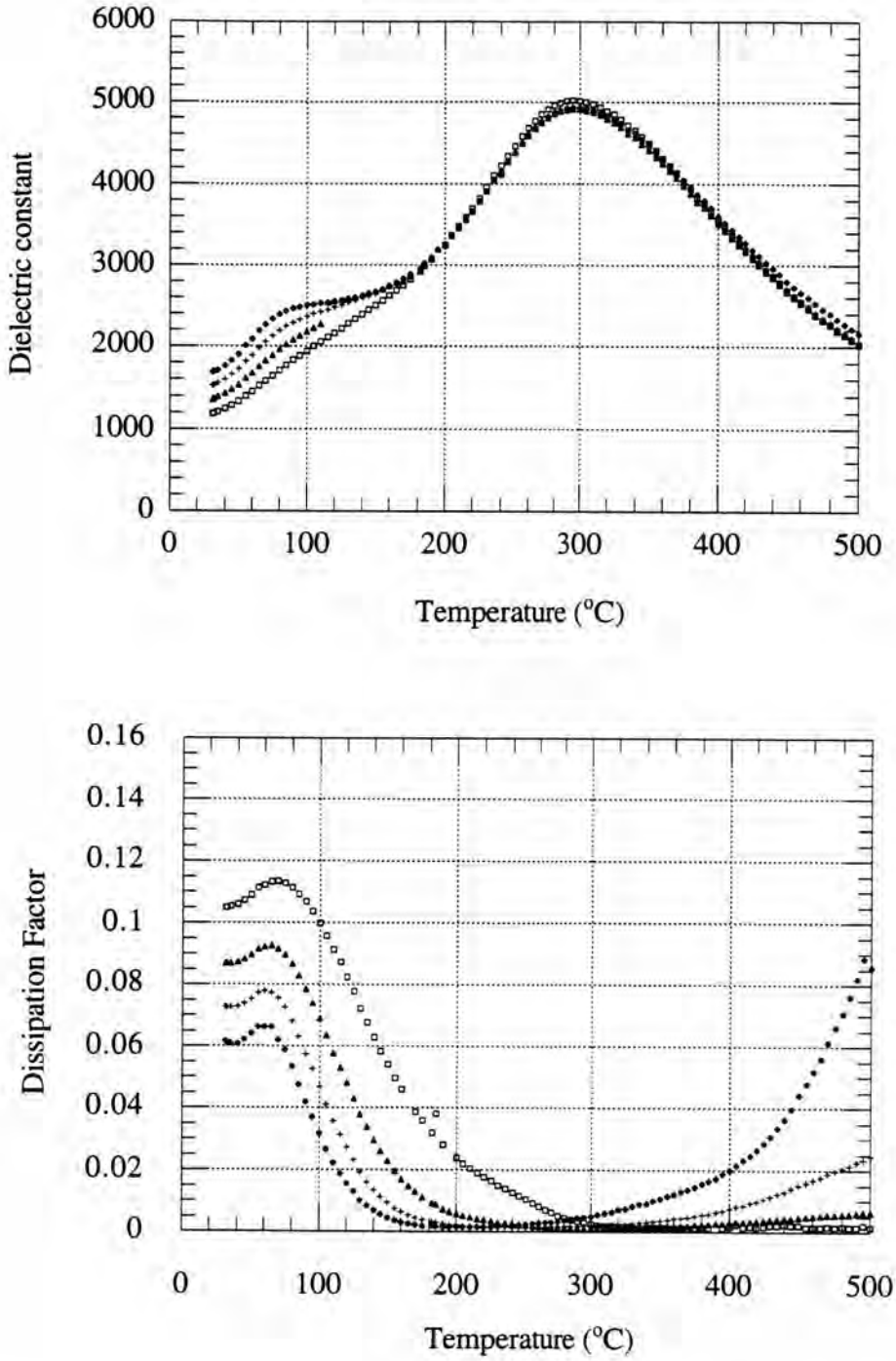

Fig.28(d) 0.85BNT-0.15BaT at 1200 °C ♦ for 1 kHz, + for 10 kHz, ▲ for 100 kHz, □ for 1 MHz

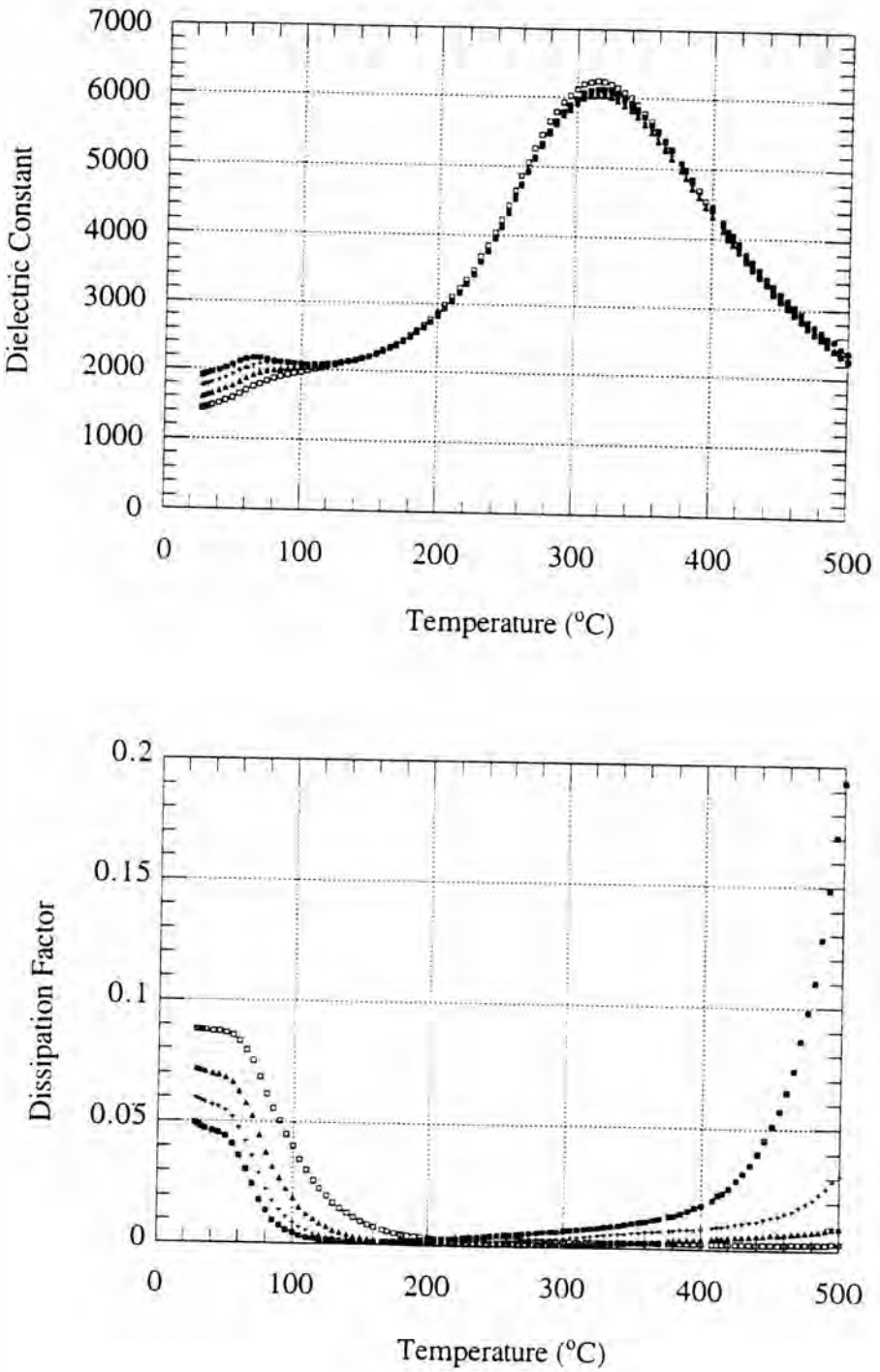

(a)

Fig.29 Change in dielectric constant and dissipation factor of (1-x)[0.90BNT -0.10PT]-xBaT at different frequencies at 1150 °C (a) x = 0.05 (b) x = 0.10 (c) x = 0.15 ♦ for 1 kHz, + for 10 kHz, ▲ for 100 kHz, □ for 1 MHz

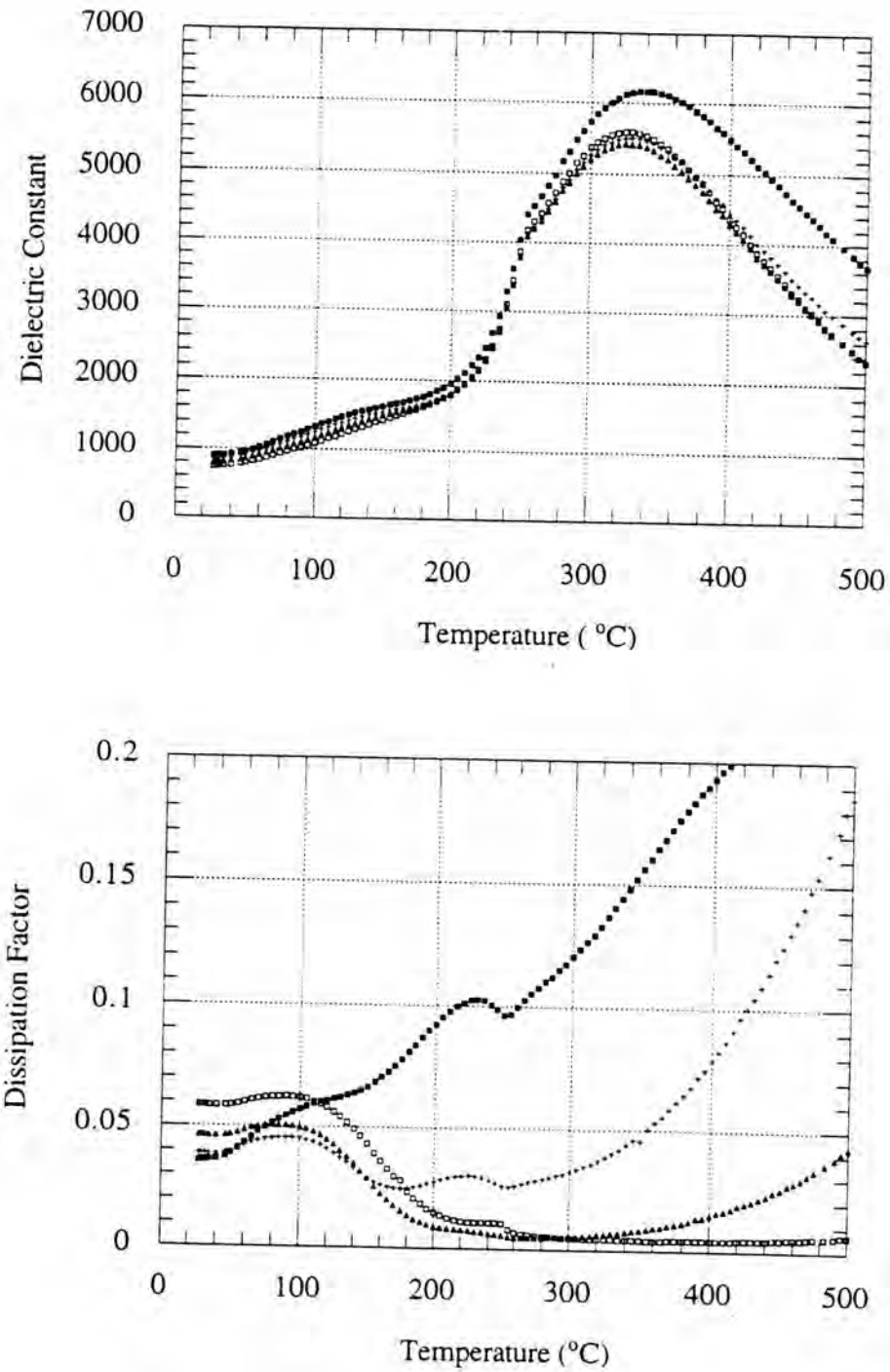

Fig.29(b) 0.90[0.90BNT-0.10PT]-0.10BaT at 1150 °C ♦ for 1 kHz, + for 10 kHz, ▲ for 100 kHz, □ for 1 MHz

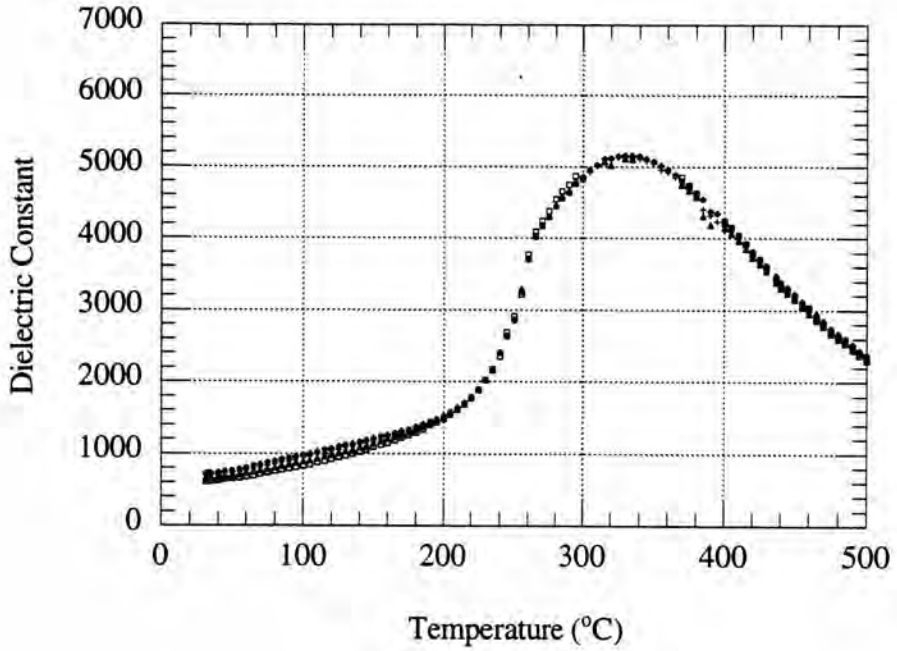

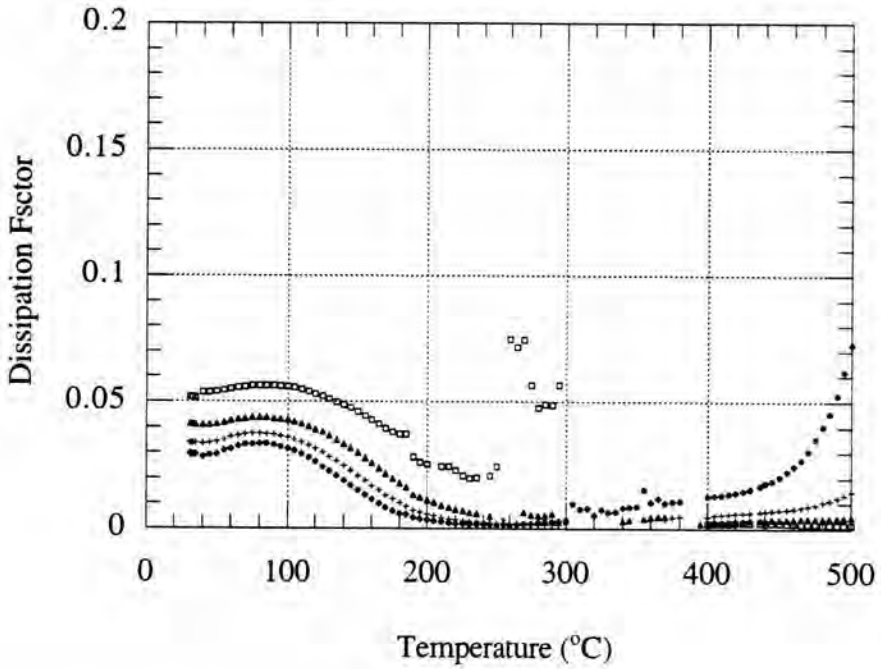

Fig.29(c) 0.85[0.90BNT-0.10PT]-0.15BaT at 1150 °C ♦ for 1 kHz, + for 10 kHz, ▲ for 100 kHz, □ for 1 MHz

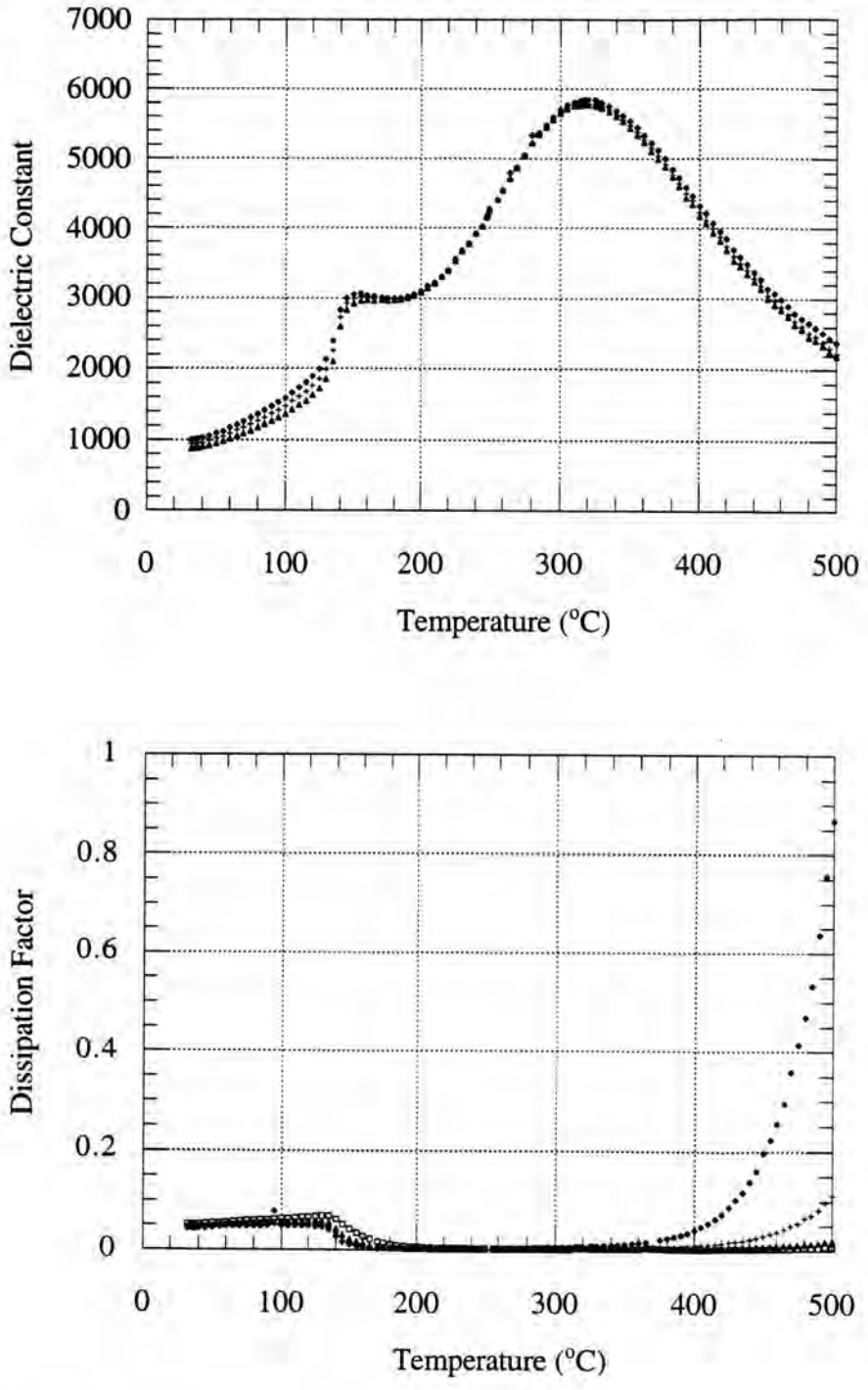

(a)

Fig.30 Change in dielectric constant and dissipation factor of (1-x)[0.90BNT-0.10PT]-xBaT at different frequencies at 1175 °C (a) x = 0.0 (b) x = 0.05 (c) x = 0.10 (d) x = 0.15 ♦ for 1 khz, + for 10 kHz, ▲ for 100 kHz, ◘ for 1 MHz

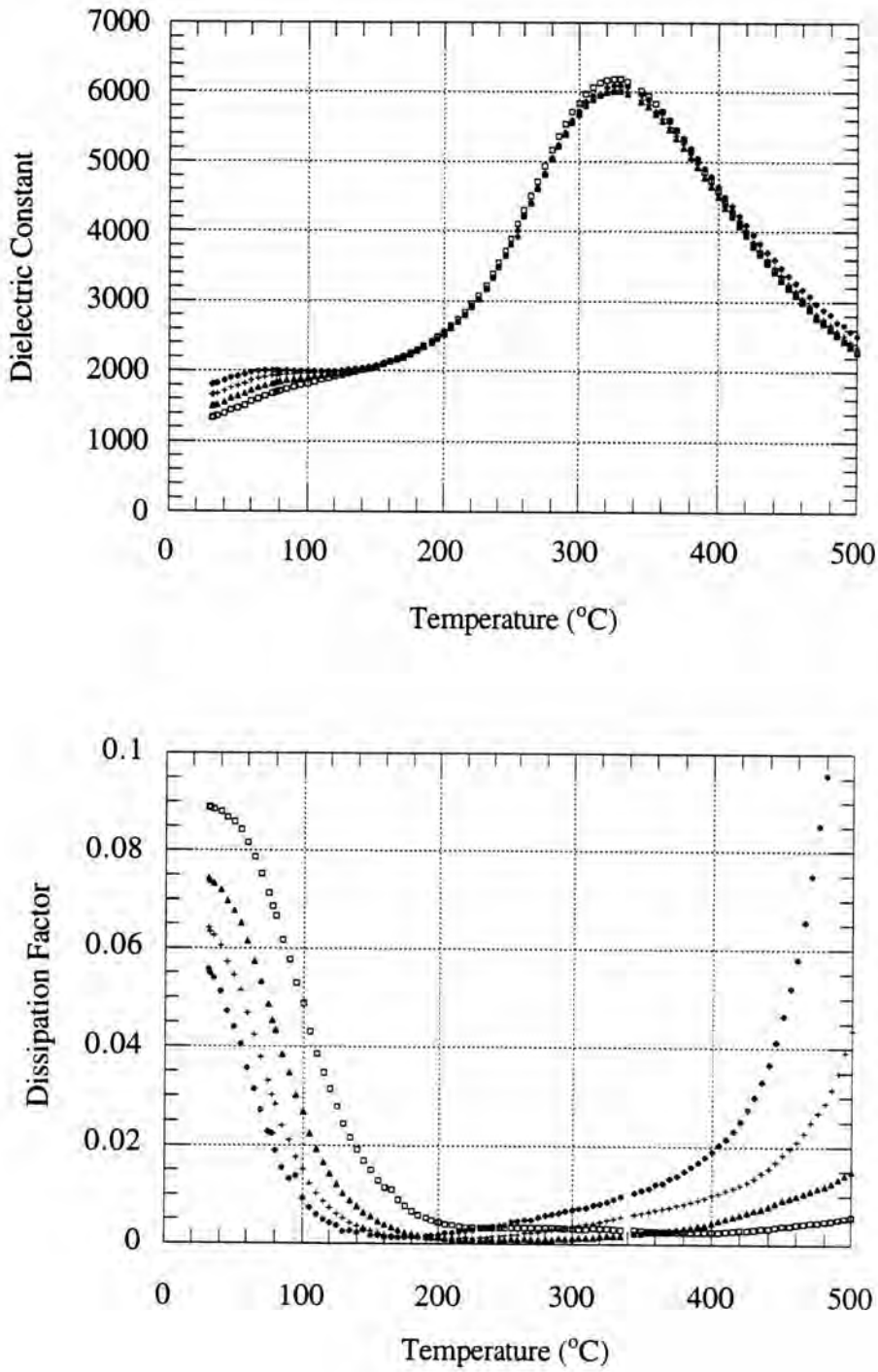

Fig.30(b) 0.95[0.90BNT-0.10PT]-0.05BaT at 1175 °C ♦ for 1 kHz, + for 10 kHz, ▲ for 100 kHz, □ for 1 MHz

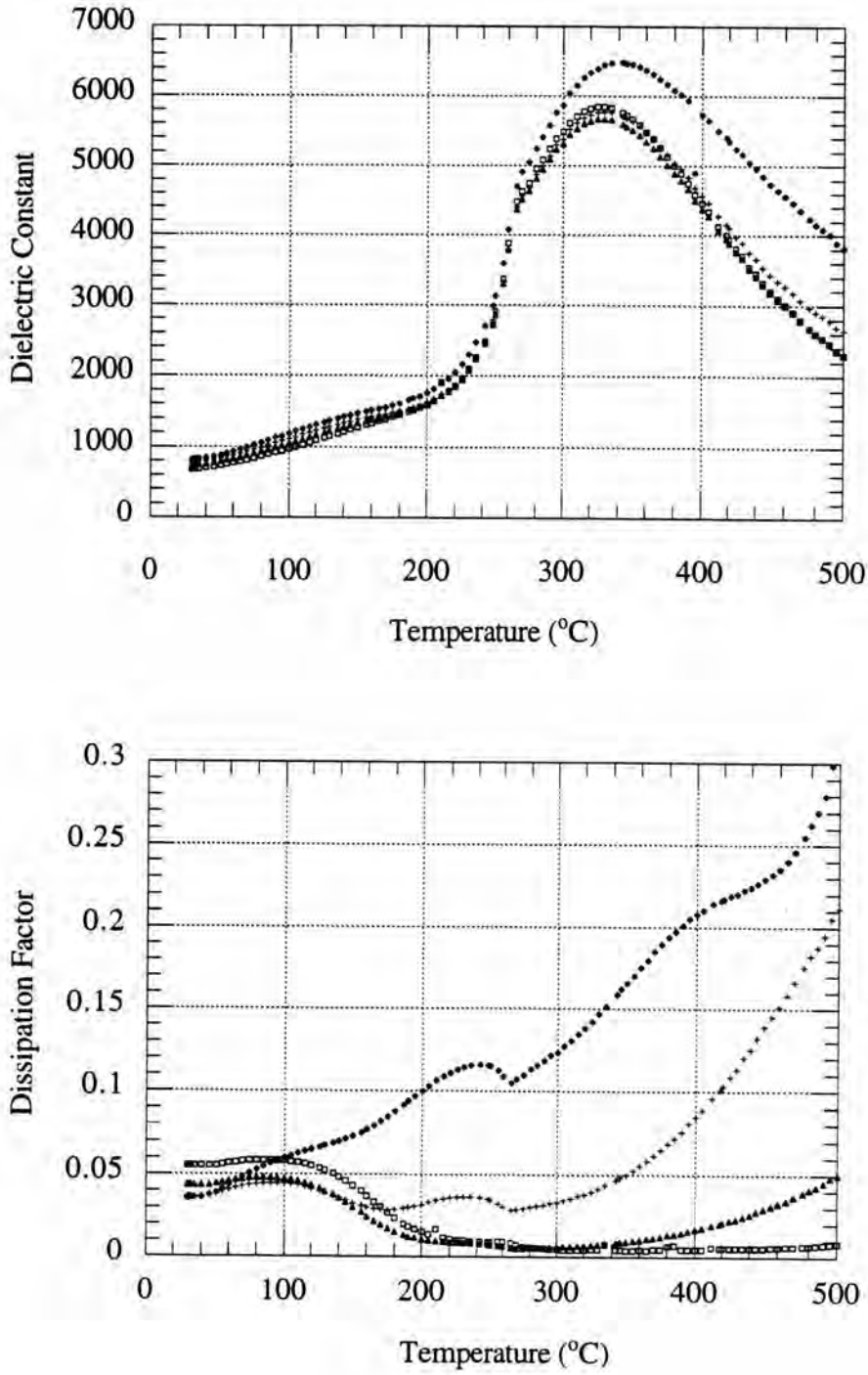

Fig.30(c) 0.90[0.90BNT-0.10PT]-0.10BaT at 1175 °C ♦ for 1 kHz, + for 10 kHz, ▲ for 100 kHz, □ for 1 MHz

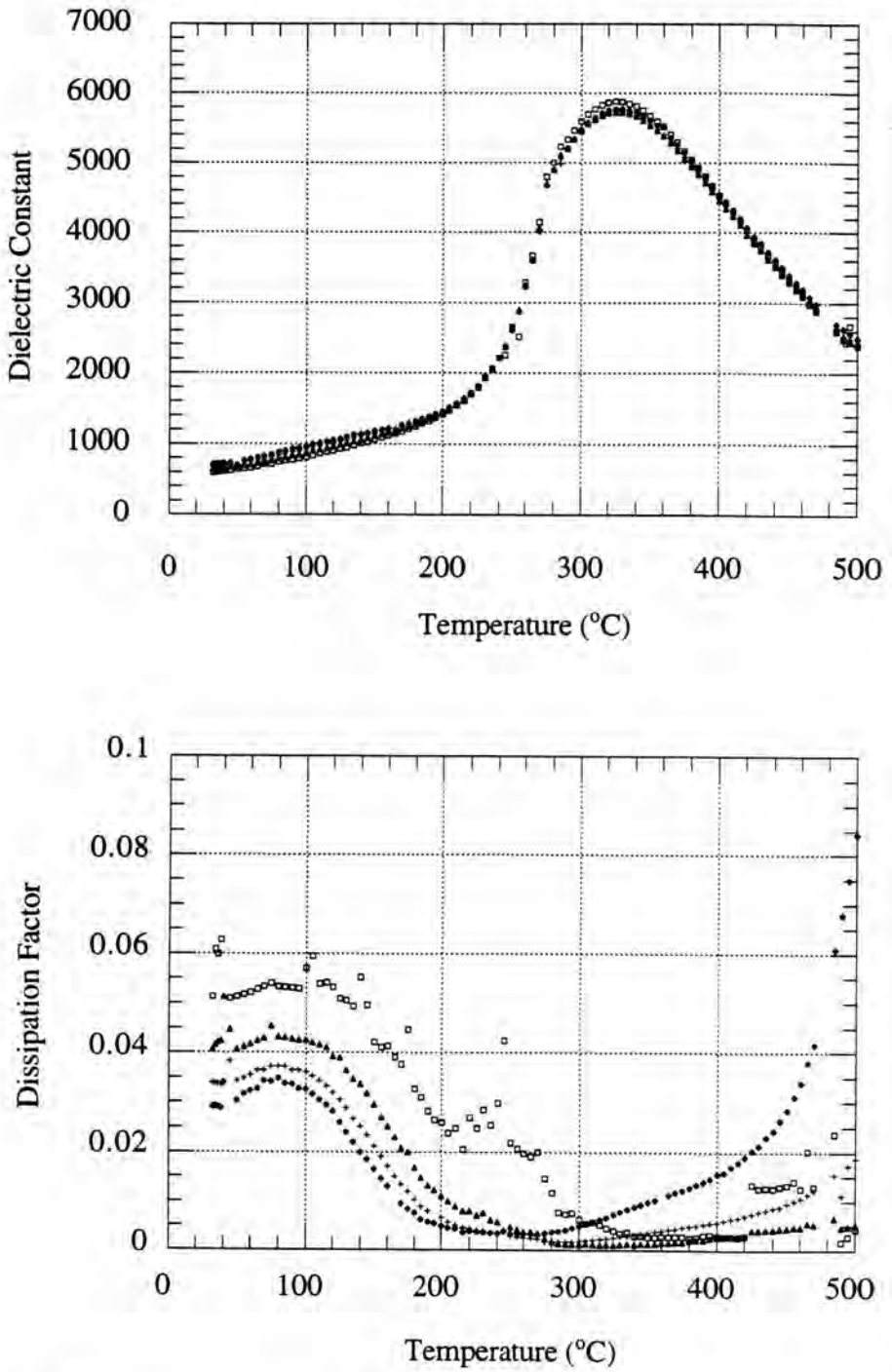

Fig.30(d) 0.85[0.90BNT-0.10PT]-0.15BaT at 1175 °C ♦ for 1 kHz, + for 10 kHz, ▲ for 100 kHz, □ for 1 MHz

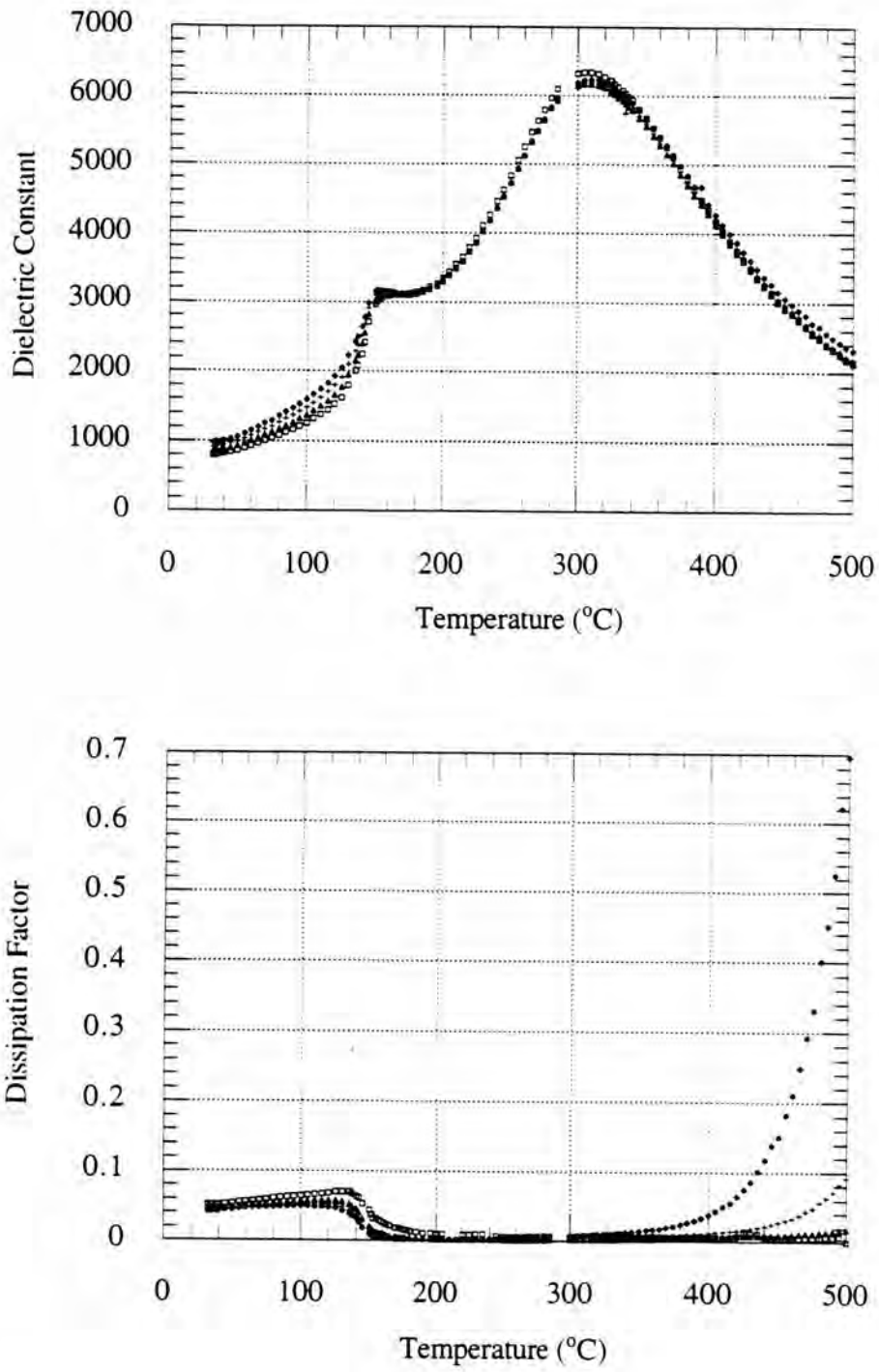

Fig.31 Change in dielectric constant and dissipation factor of (1-x)[0.90BNT -0.10PT]-xBaT at different frequencies at 1200 °C (a) x = 0.0 (b) x = 0.05 (c) x = 0.10 (d) x = 0.15 ♦ for 1 kHz, + for 10 kHz, ▲ for 100 kHz, □ for 1 MHz

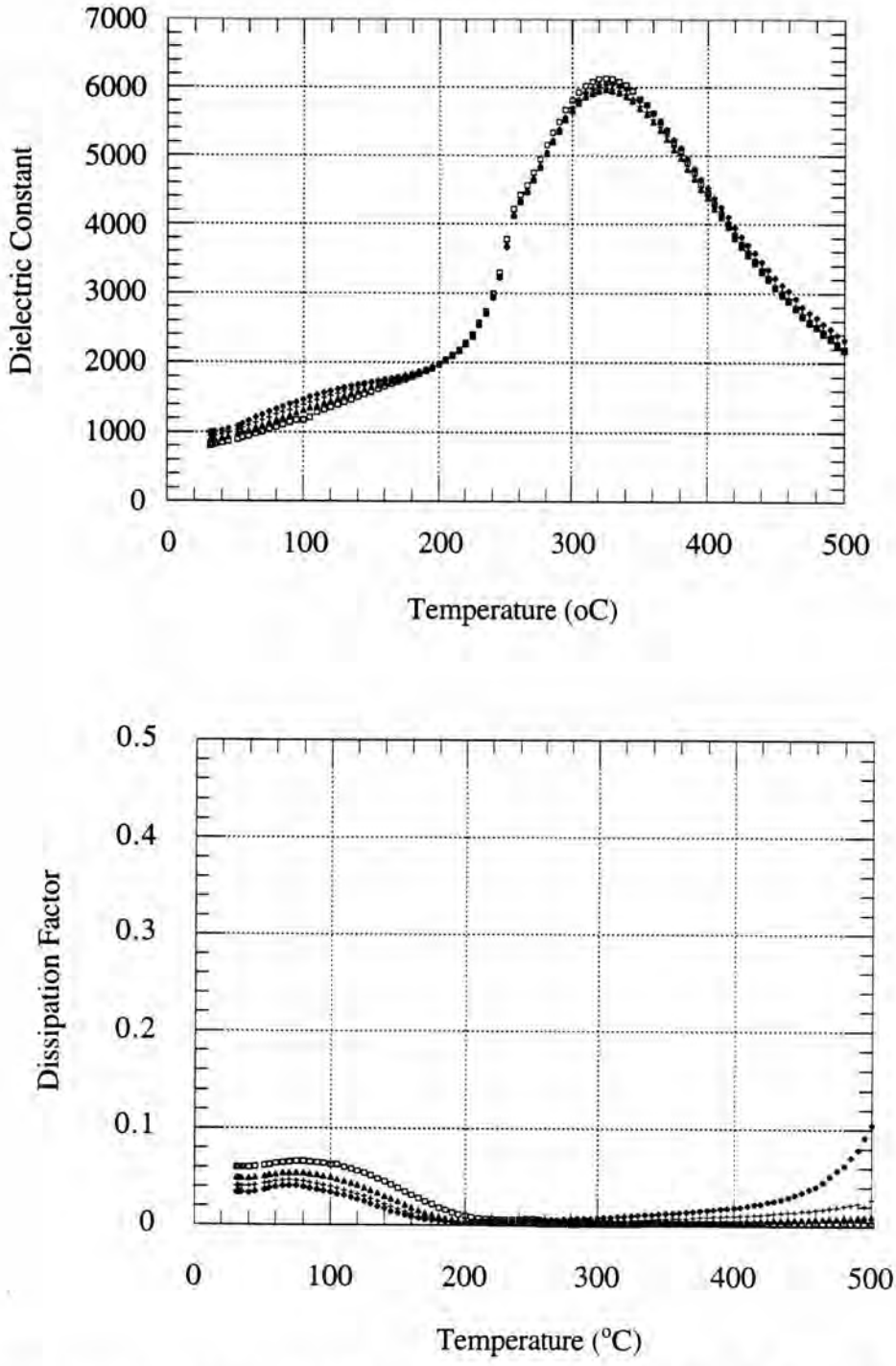

Fig.31(b) 0.95[0.90BNT-0.10PT]-0.05BaT at 1200 °C ♦ for 1 kHz, + for 10 kHZ, ▲ for 100 kHz, □ for 1 MHz

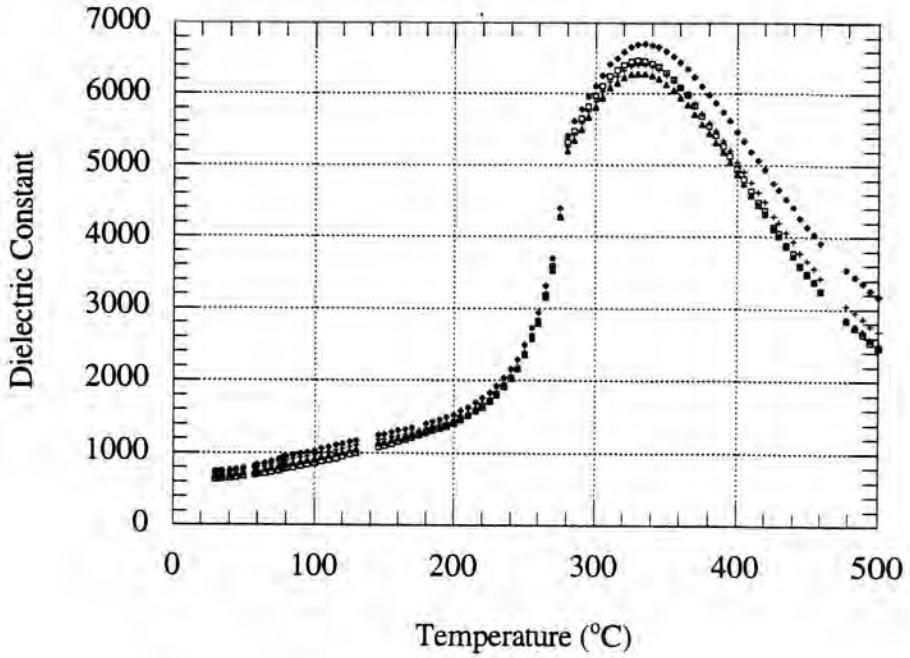

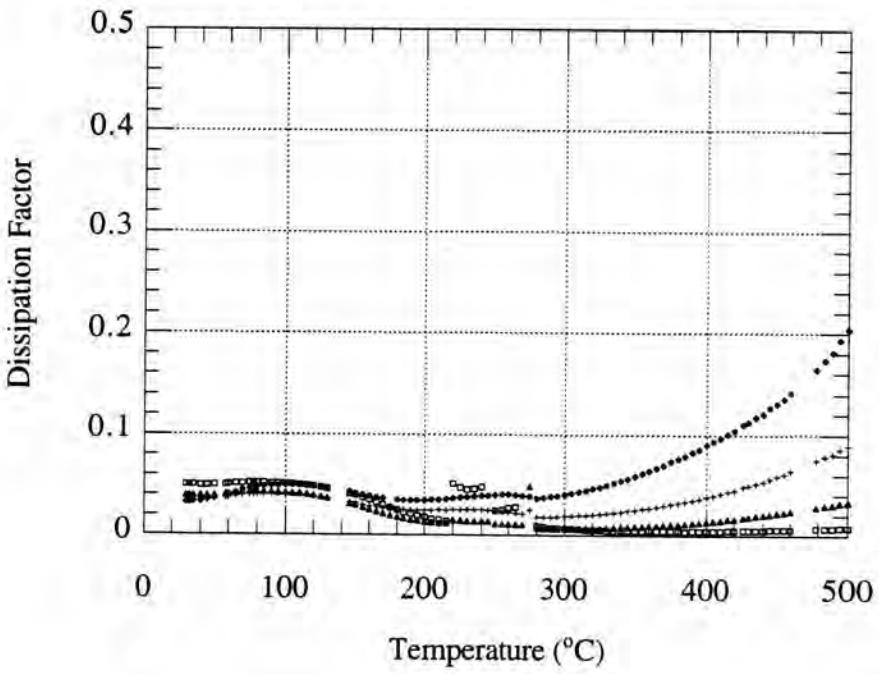

Fig.31(c) 0.90[0.90BNT-0.10PT]-0.10BaT at 1200 °C ♦ for 1 kHz, + for 10 kHz, ▲ for 100 kHz, □ for 1 MHz

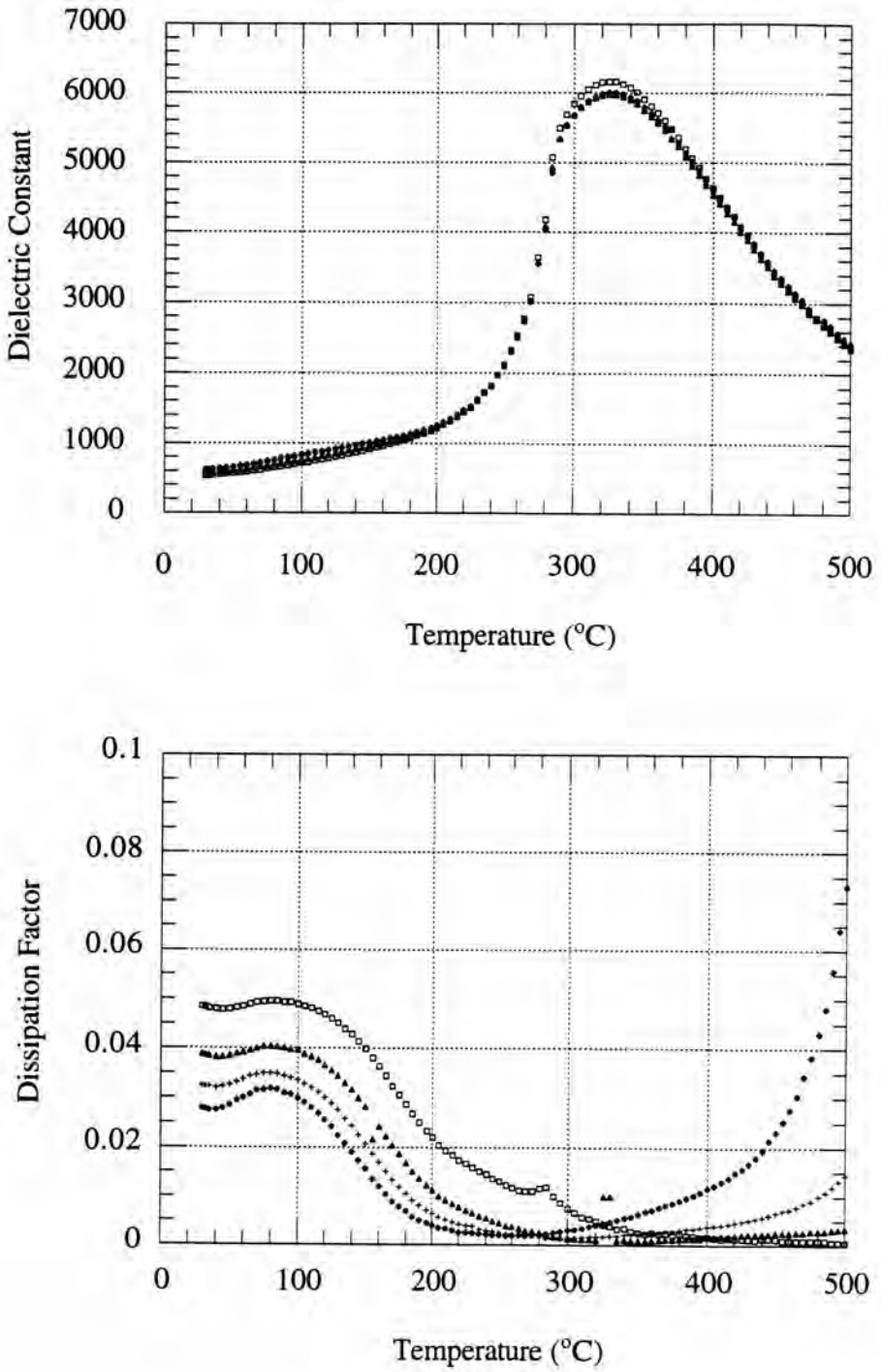

Fig.31(d) 0.85[0.90BNT-0.10PT]-0.15BaT at 1200 °C ♦ for 1 kHz, + for 10 kHz, ▲ for 100 kHz, □ for 1 MHz

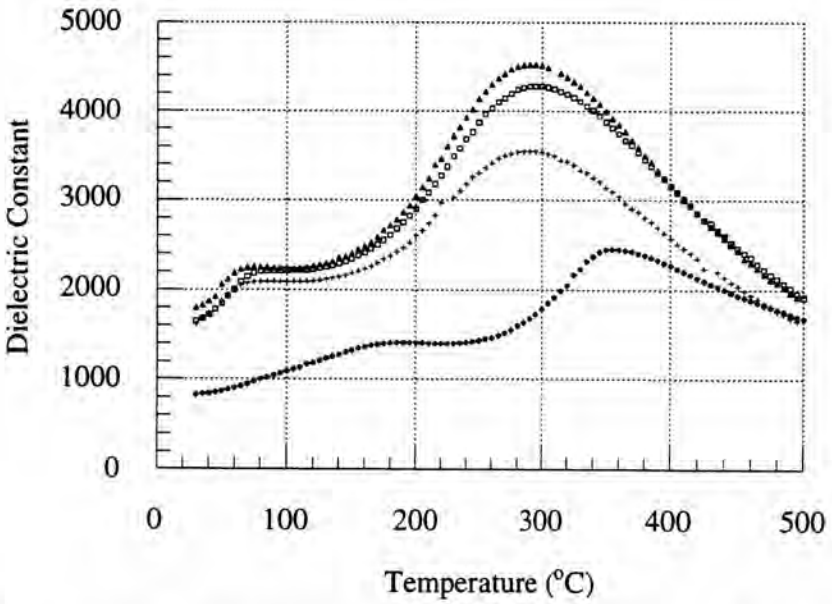

Fig.32 Change in dielectric constant of (1-x)BNT-xBaT sintered at 1175 °C temperature at 1 kHz ♦ for x = 0.0, + for x = 0.05, ▲ for x = 0.10, ◘ for x = 0.15

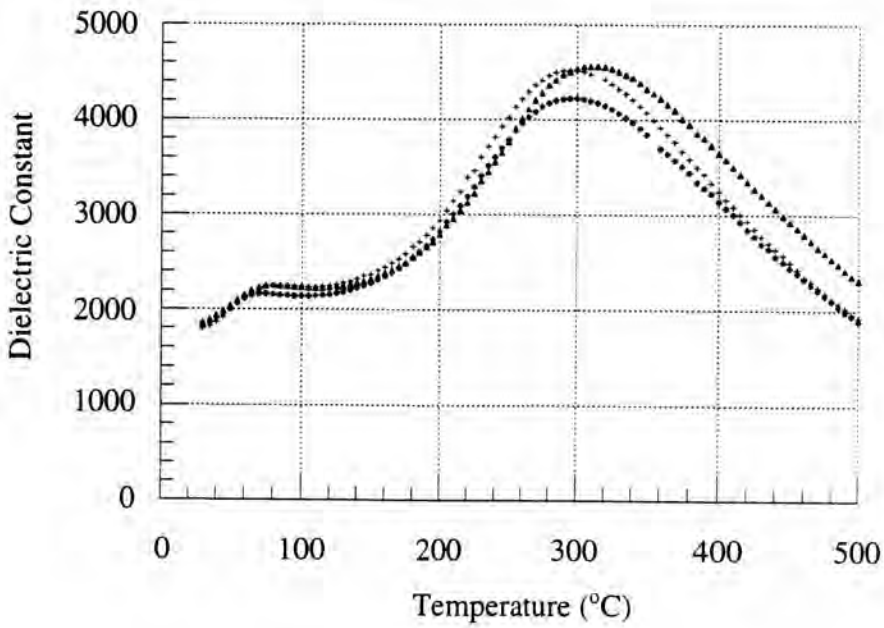

Fig.33 Change in dielectric constant of 0.90BNT-0.10BaT as a function of sintering temperature at 1 kHz ♦ for 1150 °C, + for 1175 °C, ▲ for 1200 °C

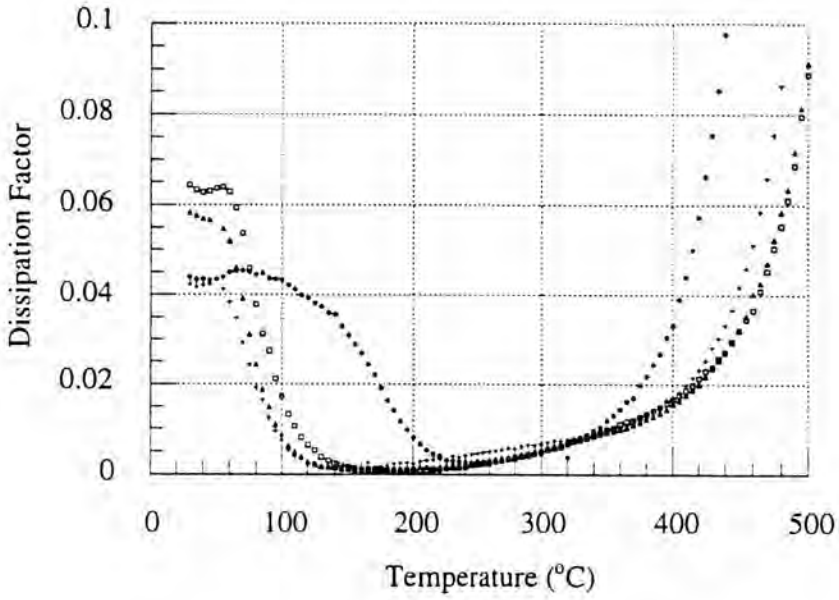

Fig.34 Change in dissipation factor (1-x)BNT-xBaT sintered at 1175 °C temperature at 1 kHz ♦ for x = 0.0, + for x = 0.05, ▲ for x = 0.10, □ for x = 0.15

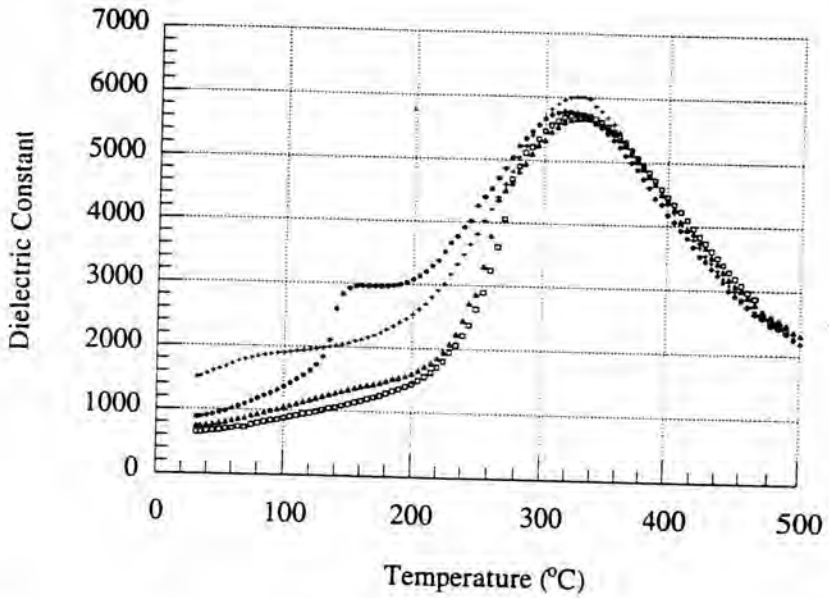

Fig.35 Change in dielectric constant of (1-x)[0.90BNT-0.10PT]-xBaT sintered at 1175 °C temperature at 100 kHz ♦ for x = 0.0, + for x = 0.05, ▲ for x = 0.10, □ for x = 0.15

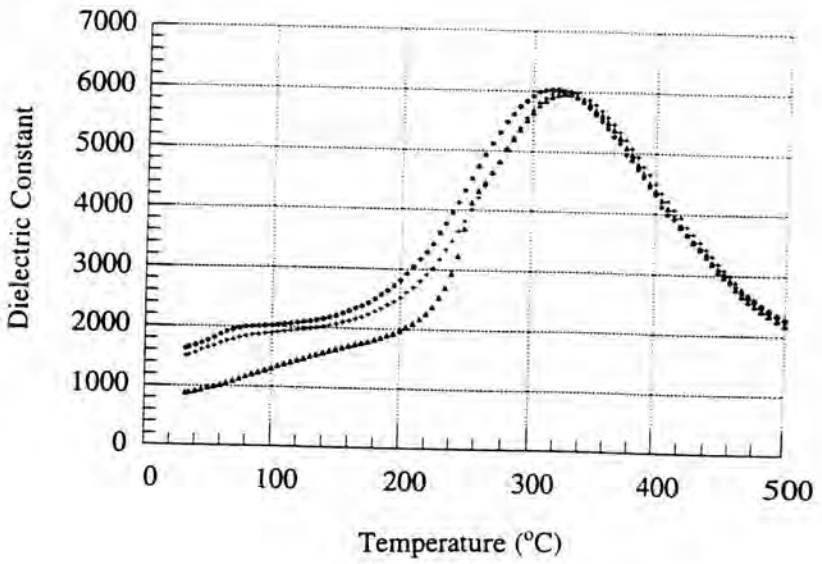

Fig.36 Change in dielectric constant of 0.95[0.90BNT-0.10PT]-0.05BaT as a function of sintering temperature at 100 kHz ♦ for 1150 °C, + for 1175 °C, ▲ for 1200 °C

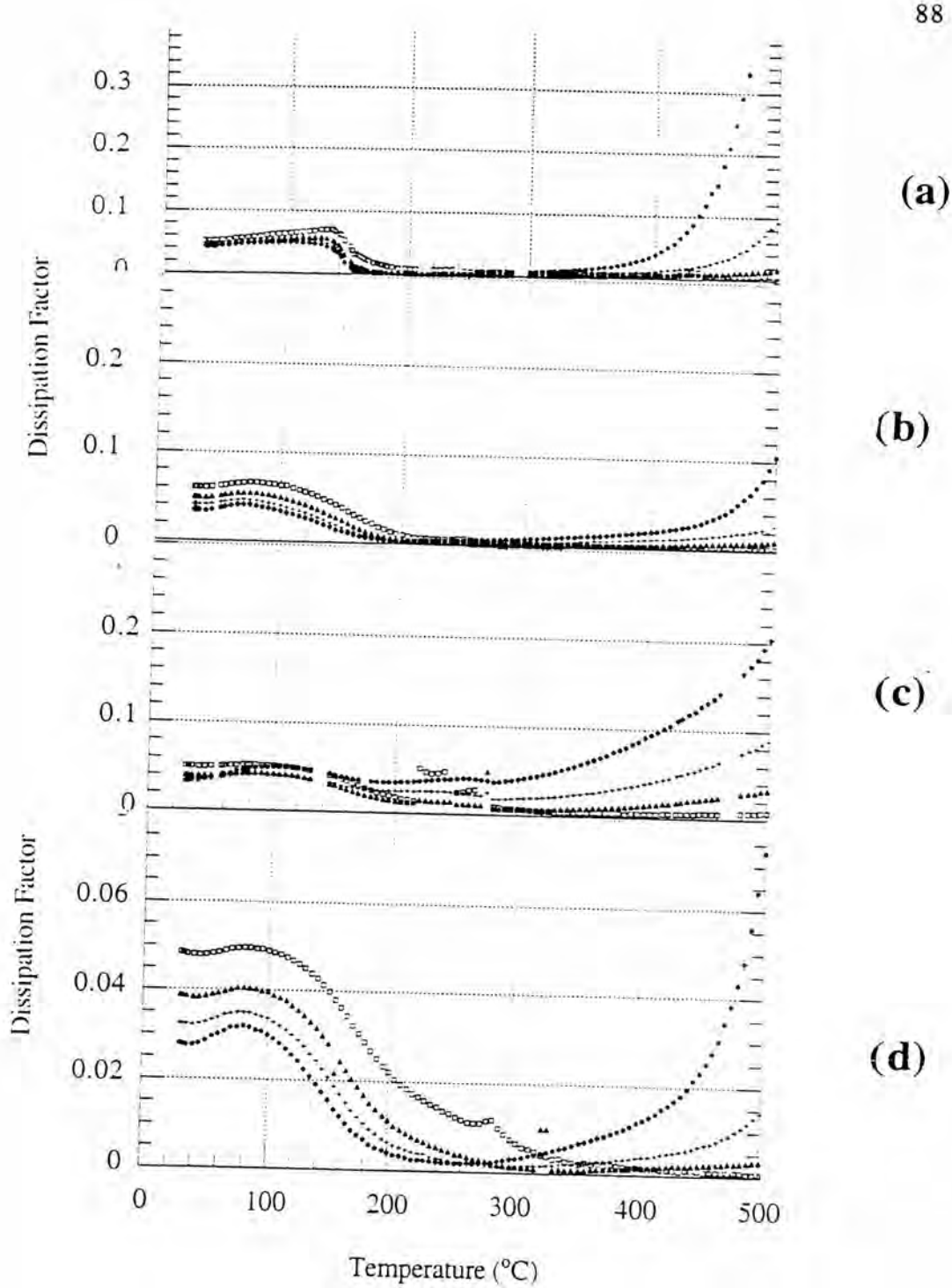

Fig.37 Change in dissipation factor of (1-x)[0.90BNT-0.10BaT]-xBaT sintered at 1175 °C temperature at different frequencies ♦ for 1 kHz, + for 10 kHz, ▲ for 100 kHz, □ for 1 MHz (a) x = 0.0 (b) x = 0.05 (c) x = 0.10 (d) x = 0.15

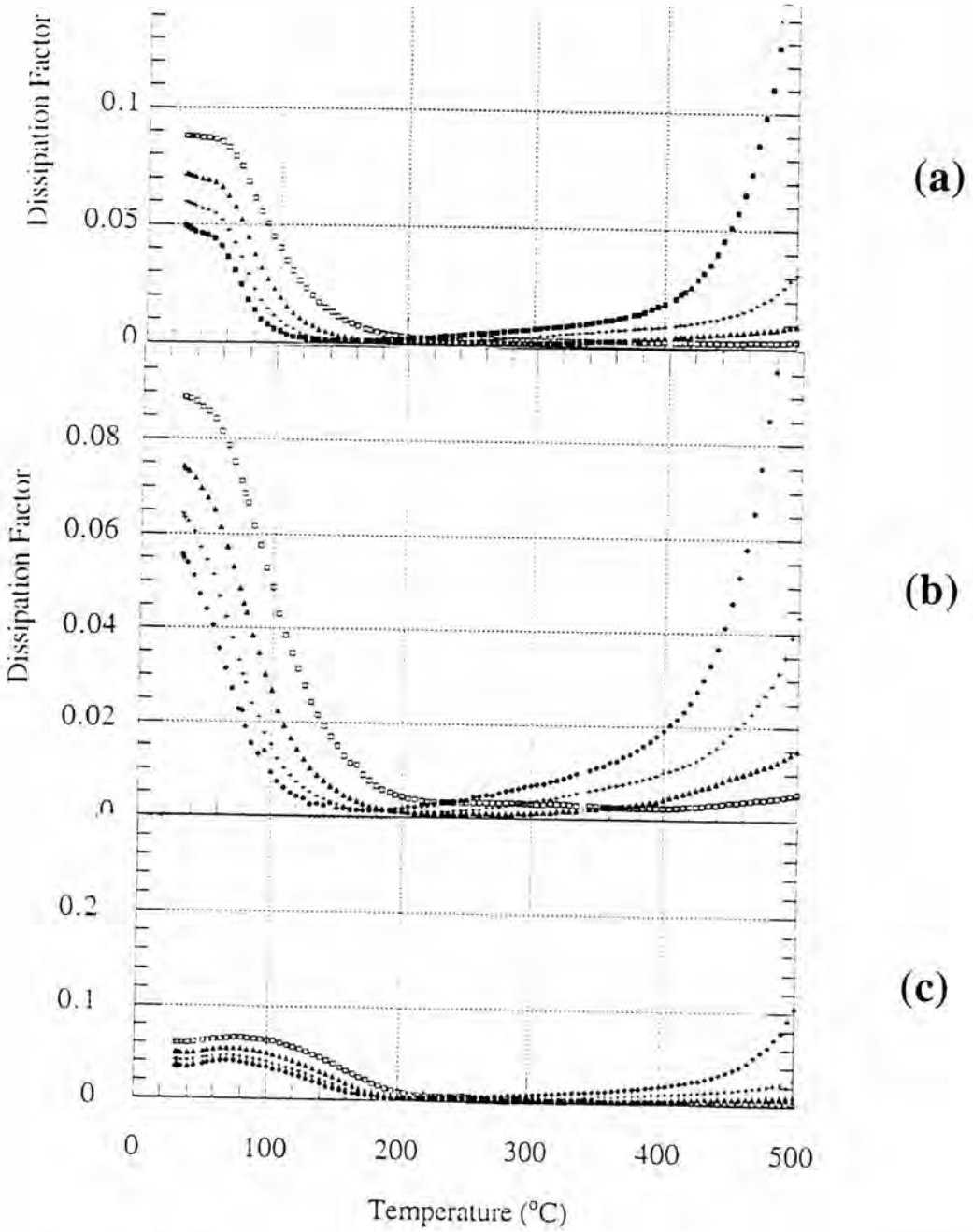

Fig.38 Change in dissipation factor of 0.95[0.90BNT-0.10PT]-0.05BaT as a function of sintering temperature at different frequencies ♦ for 1 kHz, + for 10 kHz, ▲ for 100 kHz, □ for 1 MHz (a) 1150 °C (b) 1175 °C (c) 1200 °C